

Revisiting radiative decays of single-charm baryons in the high-precision era of hadron spectroscopy

Yu-Xin Peng^{1,2,4,*}, Si-Qiang Luo^{1,2,3,4,†} and Xiang Liu^{1,2,3,4,‡}

¹*School of Physical Science and Technology, Lanzhou University, Lanzhou 730000, China*

²*Lanzhou Center for Theoretical Physics, Key Laboratory of Quantum Theory and Applications of MoE, Key Laboratory of Theoretical Physics of Gansu Province, Lanzhou University, Lanzhou 730000, China*

³*MoE Frontiers Science Center for Rare Isotopes, Lanzhou University, Lanzhou 730000, China*

⁴*Research Center for Hadron and CSR Physics, Lanzhou University & Institute of Modern Physics of CAS, Lanzhou 730000, China*

In this work, we systematically study the radiative decays of single-charm baryons, which is one aspect of their spectroscopy behavior. In order to promote the accuracy of calculations, we adopt the numerical spatial wave functions of the single-charm baryons as the theoretical input, which are obtained by the Gaussian Expansion Method for getting the mass spectrum of the single-charm baryons. The present study of hadron spectroscopy is entering the era of high precision. We believe that the present work on the radiative decays of single-charm baryons can provide valuable information for further exploration of single-charm baryons.

I. INTRODUCTION

With the experimental effort, more and more new hadronic states have been reported [1–15], witnessing the development of hadron physics in the past two decades. Among these abundant observations, single-charm baryons are a special group, as they are not only heavy-light hadronic systems, but also numerous. The observed single-charm baryons have attracted much of the hadron physics community [2, 3, 5, 9, 11].

As mentioned above, a single-charm baryon is made up of one charm quark and two light quarks, which satisfy heavy quark symmetry well. To some extent, it simplifies the study of certain properties of these particles by exploiting the fact that the heavy quark mass is much greater than the typical energy scale of the strong interactions. The study of the spectroscopy of single-charm baryons is concerned with the analysis of mass spectrum, the decay behavior and the production process. These efforts are progressively deepening our understanding of non-perturbative behavior of the strong interaction.

Focusing on over thirty single-charm baryons collected by the Particle Data Group (PDG) [16], we may notice that the observed decay modes of them not only include popular weak and strong decays, but also contain some radiative decay. For example, there are no Okubo-Zweig-Iizuka (OZI) allowed decay channels for the $\Xi_c^{\prime+}$ and $\Xi_c^{\prime0}$, the dominant decay channels being $\Xi_c^{\prime+}\gamma$ and $\Xi_c^{\prime0}\gamma$, respectively, which were observed by the CLEO Collaboration in 1998 [17]. In addition, the Ω_c^{*0} was first observed in the $\Omega_c^0\gamma$ channel by the BaBar Collaboration in 2006 [18] and confirmed by the Belle Collaboration in 2008 [19]. In 2020, the Belle Collaboration [20] observed the radiative decays of the $\Xi_c^0(2790)$ and $\Xi_c^0(2815)$ with the $\Xi_c^0\gamma$ channel. In contrast to the $\Xi_c^{\prime+}$, $\Xi_c^{\prime0}$, and Ω_c^* , this is the first observation of the radiative decays of the orbital excited single-charm baryons. These facts show that the radiative de-

cays of single-charm baryons are experimentally accessible and deserve to be studied.

There have been some theoretical investigations of this issue. We take this opportunity to briefly review the current theoretical status. In previous works, the radiative decays have been widely studied by various methods, such as light-cone QCD sum rules [21–26], heavy quark effective theory [27–29], chiral perturbation theory [30–32], constituent quark models [33–42], lattice QCD [43], relativistic quark model [44, 45], and so on. Compared to the strong decay, a typical property of the radiative decay is that the hadrons with the same isospin but contain different charges can have different decay widths. For example, the theoretical calculations show that $\text{BR}(\Xi_c^0(2790) \rightarrow \Xi_c^0\gamma) > \text{BR}(\Xi_c^+(2790) \rightarrow \Xi_c^+\gamma)$ and $\text{BR}(\Xi_c^0(2815) \rightarrow \Xi_c^0\gamma) > \text{BR}(\Xi_c^+(2815) \rightarrow \Xi_c^+\gamma)$. Such calculations are in agreement with the experimental results [20]. This implies that the radiative decays contain rich information and could provide us with useful messages to reveal the internal structures of hadrons.

The study of hadron spectroscopy is currently entering the era of high precision. In particular, with the upgrade of the high-luminosity Large Hadron Collider and the operation of Belle II, more single-charm baryons will be reported and their properties will be revealed in the future. With the promotion of experimental precision, the requirement for the theoretical precision is proposed.

Given this new situation, in this work we focus on the radiative decays of single-charm baryon, since there is still experimental potential to explore this topic. More importantly, the radiative decays of single-charm baryons are sensitive to probe the inner structure of the focused single-charm baryon. On the theoretical side, the calculated spatial wave function of the single-charm baryon is a crucial theoretical input when studying the radiative decay of single-charm baryon. Thus, this study of the radiative decays of single-charm baryon can provide a good platform to test the theoretical precision.

In Refs. [46], the Lanzhou group used the Gaussian Expansion Method (GEM), which is a high-precision method for solving few-body problems [47], to systematically study the mass spectrum of single-charm baryon family with the potential model [46, 48]. Here, the properties of these observed

*Electronic address: pengyx21@lzu.edu.cn

†Electronic address: luosq15@lzu.edu.cn

‡Electronic address: xiangliu@lzu.edu.cn

single-charm baryon were decoded and the spectroscopic behavior of the missing states was predicted. Of course, the spatial wave functions of the single-charm baryons were obtained, which form the basis of the present work.

In this work, we revisit the radiative decays of single-charm baryons. In previous work [34, 40–42], the simple harmonic oscillator wave function was usually adopted to represent the spatial wave functions of the discussed single-charm baryons. In contrast to the treatment of the spatial wave function of single-charm baryons in Refs. [34, 40–42], we take the numerical spatial wave function of single-charm baryons from the calculation by the GEM, as presented in Ref. [47]. In the next section, we will continue to compare two treatments and illustrate how these differences affect the decay width using a concrete example.

It is clear that this is timely work in anticipation of Belle II [49, 50] and Run-3 and Run-4 at LHCb [51, 52]. Although it is not easy to detect the radiative decays of single-charm baryons compared to other types of decay modes like strong decay, the present study can provide some theoretical guidance to our experimental colleagues to select some suitable radiative decays of single-charm baryon as their research topic, which will be helpful to make the corresponding observation of radiative decays of single-charm baryons become abundant. This is also the value of our work.

This paper is organized as follows. After the introduction, the deduction of the radiative decays of single-charm baryons and the details of calculation is presented in Sec. II. Then the numerical results are given in Sec. III. The paper ends with a short summary in Sec. IV.

II. RADIATIVE DECAYS OF SINGLE-CHARM BARYONS

At the tree level, the Hamiltonian of the coupling of quarks and photon is

$$H_e = - \sum_j e_j \bar{\psi}_j \gamma_\mu^j A^\mu(\mathbf{k}, \mathbf{r}) \psi_j, \quad (1)$$

where e_j , γ_μ^j , and ψ_j are the charge, Dirac matrix, and spinor of the j -th quark, respectively. A^μ in Eq. (1) is the photon field. In the non-relativistic scheme, the Hamiltonian of the coupling of quarks and photon is given by [41, 53–56]

$$h_e \simeq \sum_j \left[e_j \mathbf{r}_j \cdot \boldsymbol{\epsilon} - \frac{e_j}{2m_j} \boldsymbol{\sigma}_j \cdot (\boldsymbol{\epsilon} \times \hat{\mathbf{k}}) \right] e^{-i\mathbf{k} \cdot \mathbf{r}_j}, \quad (2)$$

where \mathbf{r}_j , m_j , and $\boldsymbol{\sigma}_j$ are the coordinate, mass, and Pauli matrix of the j -th quark, respectively. \mathbf{k} and $\boldsymbol{\epsilon}$ in Eq. (2) are the momentum and polarization vector of the photon, respectively. With the above Hamiltonian, the radiative decay amplitude is expressed as [56]

$$\mathcal{A} = -i \sqrt{\frac{\omega_\gamma}{2}} \langle f | h_e | i \rangle, \quad (3)$$

where $|i\rangle$ and $|f\rangle$ are the wave functions of the initial and final baryons, respectively. The photon energy ω_γ is defined by

$$\omega_\gamma = \frac{M_i^2 - M_f^2}{2M_i}, \quad (4)$$

where M_i and M_f are the masses of the initial and final baryons, respectively.

Finally, we can write out the general expression of the radiative decay width of single-charm baryon¹

$$\Gamma = \frac{|\mathbf{k}|^2}{\pi} \frac{2}{2J_i + 1} \frac{M_f}{M_i} \sum_{J_{fz}, J_{iz}} |\mathcal{A}_{J_{fz}, J_{iz}}|^2. \quad (5)$$

Here, J_{iz} and J_{fz} stand for the third components of the initial and final baryon angular momentum, respectively.

As shown in Eq. (3), to calculate the radiative decay widths, we need the spatial wave functions of the single-charm baryons as the input. Since a single-charm baryon contains two light flavor quarks and one heavy flavor quark, it is convenient to describe the structure in terms of heavy quark symmetry. In this scheme, the total wave function of single-charm baryon could be expressed as

$$\Psi = \sum_{n_\rho, n_\lambda} C_{n_\rho, n_\lambda} \phi^{\text{color}} \phi^{\text{flavor}} [[s_{q_1} s_{q_2}]_{s_\ell} \times [\phi_{n_\rho, l_\rho}(\boldsymbol{\rho}) \phi_{n_\lambda, l_\lambda}(\boldsymbol{\lambda})]_{L}]_{j_\ell} s_{Q_3}]_{JM}, \quad (6)$$

where $s_{q_{1(2)}}$ ($q_{1(2)} = u, d, s$) and s_{Q_3} ($Q_3 = c, b$) are the spins of the light flavor and heavy flavor quarks, respectively. l_ρ, l_λ , and L are of ρ -mode, λ -mode², and the total orbital angular momentum, respectively. s_ℓ and j_ℓ are the spin and total angular momentum of the light degree-of-freedom, respectively. ϕ^{color} is the color wave function. ϕ^{flavor} denotes the flavor wave function. In SU(3) flavor symmetry, the flavor wave functions of two light flavor quarks could be decomposed as

$$3_f \otimes 3_f = \bar{3}_f \oplus 6_f. \quad (7)$$

In the case of single-charm baryons, Λ_c^+ , Ξ_c^0 , and Ξ_c^+ belong to a irreducible representation of $\bar{3}_f$, where the flavor wave functions of two light flavor quarks are anti-symmetric. In addition, the flavor wave functions of two light flavor quarks are symmetric in a irreducible representation of 6_f , which include Σ_c^0 , Σ_c^+ , Σ_c^{++} , $\Xi_c'^0$, $\Xi_c'^+$ and Ω_c^0 .

Finally, we focus on the expression of the spatial wave function of single-charm baryon, which is related to C_{n_ρ, n_λ} , $\phi_{n_\rho, l_\rho}(\boldsymbol{\rho})$, and $\phi_{n_\lambda, l_\lambda}(\boldsymbol{\lambda})$. There are different treatments of the spatial wave functions from the different models. In the previous work [41, 46, 48, 57], it is common to use the simple harmonic oscillator (SHO) wave function to represent the spatial

¹ If we treat the quark charges as dimensionless, i.e., $e_u = \frac{2}{3}$, $e_d = -\frac{1}{3}$, $e_s = -\frac{1}{3}$, and $e_c = \frac{2}{3}$, then Eq. (5) should be multiplied by a coefficient $4\pi\alpha_{\text{EM}}$, where $\alpha_{\text{EM}} \approx \frac{1}{137}$ is the fine structure constant.

² In general, we use ρ -mode to donate the relative coordinate of the two lights, and we apply λ -mode to describe the relative position of the charmed quark and the center-of-mass of the two light quarks.

wave function, i.e.,

$$\phi_{nlm}^{\text{SHO}}(\mathbf{r}) = R_{nl}^{\text{SHO}}(\beta, r) Y_{lm}(\hat{\mathbf{r}}), \quad (8)$$

where m is the third component of the orbital angular momentum³. $R_{nl}^{\text{SHO}}(\beta, r)$ is the radial part, i.e.,

$$R_{nl}^{\text{SHO}}(\beta, r) = \beta^{l+\frac{3}{2}} \sqrt{\frac{2n!}{\Gamma(n+l+\frac{3}{2})}} e^{-\frac{\beta^2 r^2}{2}} L_n^{l+\frac{1}{2}}(\beta^2 r^2) r^l, \quad (10)$$

where β denotes the parameter in the SHO wave function. Since a single-charm baryon has two spatial degree-of-freedom, we need to introduce two parameters β_ρ and β_λ , corresponding to two SHO wave functions. Considering that each spatial degree-of-freedom has only one base, it is natural to set $C_{n_\rho, n_\lambda} = 1$, where n_ρ and n_λ are only take the radial quantum numbers in the summation.

However, we should point out that the SHO wave function is an approximate treatment of the spatial wave function of the hadron since the SHO wave function cannot be seriously considered as the eigenstate of the single-charm baryon system. Therefore, we should find another treatment to overcome this problem, which is the issue discussed in this work.

In this work, we use the GEM to solve the potential model [46, 48] and give the numerical spatial wave functions of the single-charm baryon as we did in our previous work [46]. This treatment avoids the above problem when using the SHO wave function as the input to the calculation. The Gaussian wave function is written as

$$\phi_{nlm}^{\text{Gaussian}}(\mathbf{r}) = R_{nl}^{\text{Gaussian}}(r) Y_{lm}(\hat{\mathbf{r}}), \quad (11)$$

where $R_{nl}^{\text{Gaussian}}(r)$ is the radial part with the expression

$$R_{nl}^{\text{Gaussian}}(r) = N_{nl} r^l e^{-\nu_n r^2}, \quad N_{nl} = \sqrt{\frac{2^{l+2} (2\nu_n)^{l+\frac{3}{2}}}{\sqrt{\pi} (2l+1)!!}}. \quad (12)$$

ν_n is defined by

$$\nu_n = \frac{1}{r_n^2}, \quad r_n = r_1 a^{n-1} \quad (n = 1 - n_{\max}). \quad (13)$$

In practice, we need to change the parameters $\{r_1, r_{\max}, n_{\max}\} = \{\rho_1, \rho_{\max}, n_{\max}^\rho\}$ and $\{r_1, r_{\max}, n_{\max}\} =$

³ As shown in Eq. (6), we often ignore the third components of all the angular momenta in [...]. This is an expression of the coupling scheme, which donates that there is a summation of the third component of the orbital angular momentum with Clebsch-Gordan coefficients. For the spatial wave function with total angular momentum L and third component M_L , the full expansion is

$$\begin{aligned} \psi_{LM_L}(\boldsymbol{\rho}, \boldsymbol{\lambda}) &= \sum_{n_\rho, n_\lambda} C_{n_\rho, n_\lambda} [\phi_{n_\rho, l_\rho}(\boldsymbol{\rho}) \phi_{n_\lambda, l_\lambda}(\boldsymbol{\lambda})]_{LM_L} \\ &= \sum_{n_\rho, n_\lambda} \sum_{m_\rho, m_\lambda} C_{n_\rho, n_\lambda} \langle l_\rho, m_\rho; l_\lambda, m_\lambda | LM_L \rangle \\ &\quad \times \phi_{n_\rho, l_\rho, m_\rho}(\boldsymbol{\rho}) \phi_{n_\lambda, l_\lambda, m_\lambda}(\boldsymbol{\lambda}). \end{aligned} \quad (9)$$

$\{\lambda_1, \lambda_{\max}, n_{\max}^\lambda\}$ in ρ - and λ -mode for obtaining spatial wave function of single-charm baryon. In this scheme, C_{n_ρ, n_λ} is calculated by the Rayleigh-Ritz variational method, which is a matrix⁴.

III. NUMERICAL RESULTS

In fact, there is obvious difference of two treatments when presenting the spatial wave functions dependent on ρ and λ . To illustrate this, we first present the radial parts of the wave functions, which are as follows

$$R_{l_\rho, l_\lambda}^{\text{GEM}}(\rho, \lambda) = \sum_{n_\rho, n_\lambda} C_{n_\rho, n_\lambda} R_{n_\rho, l_\rho}^{\text{Gaussian}}(\rho) R_{n_\lambda, l_\lambda}^{\text{Gaussian}}(\lambda). \quad (14)$$

$$R_{n_\rho, l_\rho, n_\lambda, l_\lambda}^{\text{SHO}}(\rho, \lambda) = R_{n_\rho, l_\rho}^{\text{SHO}}(\beta_\rho, \rho) R_{n_\lambda, l_\lambda}^{\text{SHO}}(\beta_\lambda, \lambda), \quad (15)$$

corresponding to two treatments. In general, the β_ρ and β_λ values could not be obtained directly from the concrete potential models. However, if we know the numerical spatial wave functions from solving the potential mode, the SHO parameter $\beta_{\rho, \lambda}$ could be estimated with several different approaches. With the method suggested in Refs. [46, 48, 58, 59], the $\beta_{\rho, \lambda}$ values are extracted with the spatial wave function of the GEM in Eq. (14), which is given by

$$\begin{aligned} \frac{1}{\beta_\rho^2} &= \int_0^\infty |R_{l_\rho, l_\lambda}^{\text{GEM}}(\rho, \lambda)|^2 \rho^4 \lambda^2 d\rho d\lambda, \\ \frac{1}{\beta_\lambda^2} &= \int_0^\infty |R_{l_\rho, l_\lambda}^{\text{GEM}}(\rho, \lambda)|^2 \rho^2 \lambda^4 d\rho d\lambda. \end{aligned} \quad (16)$$

Here, we take low-lying single-charm baryon $\Lambda_c^+(1S, \frac{1}{2}^+)$ as an example. In the calculations, the parameters in the GEM is employed as

$$\begin{aligned} \{\rho_1, \rho_{\max}, n_{\max}^\rho\} &= \{0.1 \text{ fm}, 5.0 \text{ fm}, 10\}, \\ \{\lambda_1, \lambda_{\max}, n_{\max}^\lambda\} &= \{0.1 \text{ fm}, 5.0 \text{ fm}, 10\}. \end{aligned} \quad (17)$$

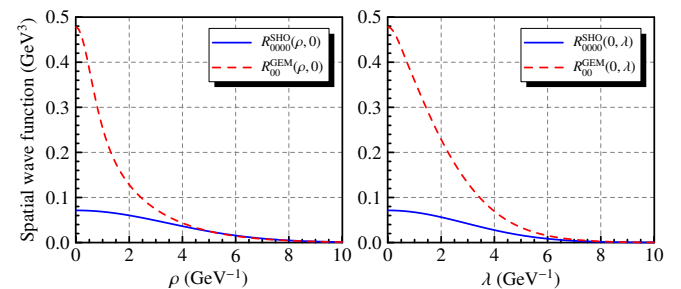


FIG. 1: The spatial wave functions $R_{n_\rho, l_\rho, n_\lambda, l_\lambda}^{\text{SHO}}(\rho, \lambda)$ and $R_{l_\rho, l_\lambda}^{\text{GEM}}(\rho, \lambda)$ dependent on ρ (left) and λ (right).

⁴ Since the single-charm baryons discussed in this work are abundant, we do not have enough space to list all the values of C_{n_ρ, n_λ} . If readers are interested in these values, they can consult Ref. [46] for more details or ours.

Then, using the Rayleigh-Ritz variational method, C_{n_ρ, n_λ} is obtained as

$$C_{n_\rho, n_\lambda} = 10^{-3} \times \begin{pmatrix} -0.093 & 0.689 & -0.687 & 2.178 & 4.442 & 4.688 & -0.876 & 0.391 & -0.155 & 0.039 \\ 2.085 & -4.407 & 9.332 & -2.680 & 33.777 & 21.436 & -2.020 & 0.612 & -0.159 & 0.024 \\ -0.973 & 9.959 & -15.248 & 27.579 & 22.564 & 36.328 & -8.591 & 4.093 & -1.698 & 0.438 \\ -1.737 & -0.326 & 32.856 & -32.591 & 89.858 & 37.447 & 0.736 & -1.416 & 0.858 & -0.268 \\ 3.663 & -12.114 & 7.243 & 94.438 & 46.207 & 87.520 & -22.094 & 10.581 & -4.360 & 1.111 \\ -3.269 & 12.907 & -24.201 & 3.425 & 367.804 & 201.317 & -20.484 & 6.643 & -2.013 & 0.398 \\ 2.771 & -11.889 & 28.970 & -50.831 & 62.840 & 203.767 & -36.996 & 16.537 & -6.458 & 1.579 \\ -1.385 & 5.842 & -13.721 & 22.097 & -19.483 & -37.457 & 9.740 & -4.572 & 1.870 & -0.474 \\ 0.609 & -2.541 & 5.867 & -9.182 & 7.537 & 12.288 & -3.246 & 1.554 & -0.647 & 0.167 \\ -0.164 & 0.680 & -1.548 & 2.381 & -1.922 & -2.743 & 0.729 & -0.353 & 0.149 & -0.039 \end{pmatrix}, \quad (18)$$

where n_ρ and n_λ are the row and column indices, respectively. With the coefficients obtained above, one obtains $\beta_\rho = 0.290$ GeV and $\beta_\rho = 0.344$ GeV in the SHO wave function (see Eq. (15)) for the $\Lambda_c^+(1S, \frac{1}{2}^+)$.

We note that both $R_{n_\rho, n_\lambda}^{\text{SHO}}(\rho, \lambda)$ and $R_{l_\rho, l_\lambda}^{\text{GEM}}(\rho, \lambda)$ are two-dimensional functions. To plot the curves conveniently, we set $\rho = 0$ or $\lambda = 0$ and obtain the functions depending on another variation. Here, we employ the $\Lambda_c^+(1S)$ as an example. The results are presented in Fig. 1. According to Fig. 1, there are obvious differences between the SHO and GEM wave functions.

In the following discussions, we take the numerical spatial wave functions of single-charm baryons from the potential model solved by the GEM [46], which are used as input to calculate their radiative decay behaviors. These involved single-charm baryons are collected in Table I. The results match the PDG [16] and previous studies [58, 60–66].

A. $\bar{3}_f \rightarrow 1S + \gamma$

Among these decay channels of $\bar{3}_f$ single-charm baryons, we first consider the simplest situation, i.e., $\bar{3}_f \rightarrow 1S + \gamma$, where the $1S$ stands for the $\Lambda_c(1S)$, $\Sigma_c(1S)$, and $\Xi_c^{(\prime)}(1S)$ states. The numerical results are presented in Table II.

For the $\Lambda_c^+(1P)$, the radiative decay widths of the $\Lambda_c^+(1S)/\Sigma_c(1S)\gamma$ modes are very small, where similar results are also obtained in Refs. [34, 41]. Thus, the experimental detection of these decay channels experimentally are a real challenge. But for the $\Lambda_c^+(1D)$, the $\Lambda_c^+(1D, \frac{3}{2}^+) \rightarrow \Lambda_c^+(1S, \frac{1}{2}^+)\gamma$ and $\Lambda_c^+(1D, \frac{3}{2}^+) \rightarrow \Lambda_c^+(1S, \frac{1}{2}^+)\gamma$ channels have considerable decay widths. We therefore suggest that the experimental colleague could concentrate on the radiative decays of the $\Lambda_c^+(1D, \frac{3}{2}^+)$ and $\Lambda_c^+(1D, \frac{5}{2}^+)$. However, the radiative decay widths of the $\Lambda_c^+(1F)/\Lambda_c(2S)$ transitions into $\Lambda_c^+(1S)/\Sigma_c^+(1S)\gamma$ are very small, which shows that finding

them is also a difficult task for experiments.

The Ξ_c states contain two charge status, i.e., Ξ_c^0 and Ξ_c^+ . In radiative decays, the Ξ_c^0 and Ξ_c^+ have significantly different properties. A typical example is the different decay widths of $\Xi_c^0(1P, \frac{1}{2}^-)/\Xi_c^0(1P, \frac{3}{2}^-) \rightarrow \Xi_c^0(1S, \frac{1}{2}^+)\gamma$ and $\Xi_c^+(1P, \frac{1}{2}^-)/\Xi_c^+(1P, \frac{3}{2}^-) \rightarrow \Xi_c^+(1S, \frac{1}{2}^+)\gamma$. For the $\Xi_c^0(1P, \frac{1}{2}^-)/\Xi_c^0(1P, \frac{3}{2}^-) \rightarrow \Xi_c^0(1S, \frac{1}{2}^+)\gamma$ transitions, the theoretical widths are about 200 keV, while the widths of $\Xi_c^+(1P, \frac{1}{2}^-)/\Xi_c^+(1P, \frac{3}{2}^-) \rightarrow \Xi_c^+(1S, \frac{1}{2}^+)\gamma$ are only of the order of a few keV. Similar results are also obtained in Refs. [34, 41]. This could explain why the Belle Collaboration [20] successfully measured the relative branching ratios of $\Xi_c^0(1P, \frac{1}{2}^-)/\Xi_c^0(1P, \frac{3}{2}^-) \rightarrow \Xi_c^0(1S, \frac{1}{2}^+)\gamma$ with $\Xi_c^0(1P, \frac{1}{2}^-)/\Xi_c^0(1P, \frac{3}{2}^-) \rightarrow \Xi_c^{+\prime}(1S, \frac{1}{2}^+)\pi^-/\Xi_c^{*+}(1S, \frac{3}{2}^+)\pi^- \rightarrow \Xi_c^+(1S, \frac{1}{2}^+)\gamma\pi^-/\Xi_c^+(1S, \frac{1}{2}^+)\pi^+\pi^-$, but only give upper branch ratio limits of $\Xi_c^+(1P, \frac{1}{2}^-)/\Xi_c^+(1P, \frac{3}{2}^-) \rightarrow \Xi_c^+(1S, \frac{1}{2}^+)\gamma$ with $\Xi_c^+(1P, \frac{1}{2}^-)/\Xi_c^+(1P, \frac{3}{2}^-) \rightarrow \Xi_c^{0\prime}(1S, \frac{1}{2}^+)\pi^+/\Xi_c^{*0}(1S, \frac{3}{2}^+)\pi^+ \rightarrow \Xi_c^0(1S, \frac{1}{2}^+)\gamma\pi^+/\Xi_c^+(1S, \frac{1}{2}^+)\pi^+\pi^+$. On the other hand, if we treat the light flavor-spatial wave functions of Ξ_c as antisymmetrical and Ξ_c' as symmetric, the couplings between the Ξ_c^0 and $\Xi_c^{0\prime}\gamma$ are forbidden, since the the charge expectations satisfy $\langle e_1 \rangle = \langle e_2 \rangle = \langle e_3 \rangle = 0$. If we consider the small constituent quark mass gap of $m_d - m_s$, the decays are allowed. But in general, the decay widths are suppressed, i.e., most of the calculated results are less than 0.1 keV as shown in Table II. According to Table II we also find that some decay channels can have significant radiative decay widths, including $\Xi_c^{0,+}(1D) \rightarrow \Xi_c^{0,+}(1S)\gamma$ and $\Xi_c^0(1F) \rightarrow \Xi_c^0(1S)\gamma$. However, for other radiative decay processes in Table II, the calculated widths are about or less than 1 keV.

TABLE I: Mass spectrum of single-charm baryons [16, 46]. The masses of the well-established states in the PDG [16] are in bold, while the unbolded masses are theoretical results from Ref. [46].

States	I_ρ	I_λ	L	s_ℓ	j_ℓ	J	M (MeV)
$\Lambda_c/\Xi_c(1S, \frac{1}{2}^+)$	0	0	0	0	0	$\frac{1}{2}$	2286/2470
$\Lambda_c/\Xi_c(1P, \frac{1}{2}^-)$	0	1	1	0	1	$\frac{1}{2}$	2592/2790
$\Lambda_c/\Xi_c(1P, \frac{3}{2}^-)$	0	1	1	0	1	$\frac{3}{2}$	2628/2820
$\Lambda_c/\Xi_c(1D, \frac{3}{2}^+)$	0	2	2	0	2	$\frac{3}{2}$	2856/3056
$\Lambda_c/\Xi_c(1D, \frac{5}{2}^+)$	0	2	2	0	2	$\frac{5}{2}$	2882/3075
$\Lambda_c/\Xi_c(1F, \frac{5}{2}^-)$	0	3	3	0	3	$\frac{5}{2}$	3075/3292
$\Lambda_c/\Xi_c(1F, \frac{7}{2}^-)$	0	3	3	0	3	$\frac{7}{2}$	3079/3295
$\Lambda_c/\Xi_c(2S, \frac{1}{2}^+)$	0	0	0	0	0	$\frac{1}{2}$	2767/2970
$\Sigma_c/\Xi'_c/\Omega_c(1S, \frac{1}{2}^+)$	0	0	0	1	1	$\frac{1}{2}$	2455/2580/2695
$\Sigma_c^*/\Xi_c^*/\Omega_c^*(1S, \frac{3}{2}^+)$	0	0	0	1	1	$\frac{3}{2}$	2520/2645/2766
$\Sigma_{c0}/\Xi'_{c0}/\Omega_{c0}(1P, \frac{1}{2}^-)$	0	1	1	1	0	$\frac{1}{2}$	2785/2919/3030
$\Sigma_{c1}/\Xi'_{c1}/\Omega_{c1}(1P, \frac{1}{2}^-)$	0	1	1	1	1	$\frac{1}{2}$	2771/2906/3020
$\Sigma_{c1}/\Xi'_{c1}/\Omega_{c1}(1P, \frac{3}{2}^-)$	0	1	1	1	1	$\frac{3}{2}$	2798/2938/3056
$\Sigma_{c2}/\Xi'_{c2}/\Omega_{c2}(1P, \frac{3}{2}^-)$	0	1	1	1	2	$\frac{3}{2}$	2780/2927/3053
$\Sigma_{c2}/\Xi'_{c2}/\Omega_{c2}(1P, \frac{5}{2}^-)$	0	1	1	1	2	$\frac{5}{2}$	2797/2945/3073
$\Sigma_{c1}/\Xi'_{c1}/\Omega_{c1}(1D, \frac{1}{2}^+)$	0	2	2	1	1	$\frac{1}{2}$	3043/3186/3298
$\Sigma_{c1}/\Xi'_{c1}/\Omega_{c1}(1D, \frac{3}{2}^+)$	0	2	2	1	1	$\frac{3}{2}$	3058/3201/3315
$\Sigma_{c2}/\Xi'_{c2}/\Omega_{c2}(1D, \frac{3}{2}^+)$	0	2	2	1	2	$\frac{3}{2}$	3031/3181/3303
$\Sigma_{c2}/\Xi'_{c2}/\Omega_{c2}(1D, \frac{5}{2}^+)$	0	2	2	1	2	$\frac{5}{2}$	3043/3194/3317
$\Sigma_{c3}/\Xi'_{c3}/\Omega_{c3}(1D, \frac{5}{2}^+)$	0	2	2	1	3	$\frac{5}{2}$	3010/3173/3307
$\Sigma_{c3}/\Xi'_{c3}/\Omega_{c3}(1D, \frac{7}{2}^+)$	0	2	2	1	3	$\frac{7}{2}$	3017/3179/3314
$\Sigma_{c2}/\Xi'_{c2}/\Omega_{c2}(1F, \frac{3}{2}^-)$	0	3	3	1	2	$\frac{3}{2}$	3277/3427/3540
$\Sigma_{c2}/\Xi'_{c2}/\Omega_{c2}(1F, \frac{5}{2}^-)$	0	3	3	1	2	$\frac{5}{2}$	3283/3433/3546
$\Sigma_{c3}/\Xi'_{c3}/\Omega_{c3}(1F, \frac{3}{2}^-)$	0	3	3	1	3	$\frac{3}{2}$	3247/3408/3532
$\Sigma_{c3}/\Xi'_{c3}/\Omega_{c3}(1F, \frac{5}{2}^-)$	0	3	3	1	3	$\frac{5}{2}$	3252/3412/3536
$\Sigma_{c4}/\Xi'_{c4}/\Omega_{c4}(1F, \frac{7}{2}^-)$	0	3	3	1	4	$\frac{7}{2}$	3208/3383/3521
$\Sigma_{c4}/\Xi'_{c4}/\Omega_{c4}(1F, \frac{9}{2}^-)$	0	3	3	1	4	$\frac{9}{2}$	3209/3383/3521
$\Sigma_c/\Xi'_c/\Omega_c(2S, \frac{1}{2}^+)$	0	0	0	1	1	$\frac{1}{2}$	2947/3090/3203
$\Sigma_c^*/\Xi_c^*/\Omega_c^*(2S, \frac{3}{2}^+)$	0	0	0	1	1	$\frac{3}{2}$	2979/3124/3243

B. $6_f \rightarrow 1S + \gamma$

In the radiative decay processes of 6_f single-charm baryons, we also calculate the widths of radiative decays with final states $\Lambda_c(1S)/\Sigma_c(1S)/\Xi_c^{(\prime)}(1S)/\Omega_c(1S)\gamma$ as the prior. The numerical results are given in Table III.

In the radiative decays of $\Sigma_c(1S)$, we find that $\Sigma_c^+(1S, \frac{1}{2}^+) \rightarrow \Lambda_c^+(1S, \frac{1}{2}^+)\gamma$ and $\Sigma_c^{*+}(1S, \frac{3}{2}^+) \rightarrow \Lambda_c^+(1S, \frac{1}{2}^+)\gamma$ have considerable decay widths. Since the $\Lambda_c^+(1S, \frac{1}{2}^+)$ is well established, it is possible to observe the two processes mentioned above. But the radiative decay widths of $\Sigma_c^{*0}(1S, \frac{3}{2}^+) \rightarrow \Sigma_c^0(1S, \frac{1}{2}^+)\gamma$, $\Sigma_c^{*+}(1S, \frac{3}{2}^+) \rightarrow \Sigma_c^+(1S, \frac{1}{2}^+)\gamma$, and $\Sigma_c^{*++}(1S, \frac{3}{2}^+) \rightarrow \Sigma_c^{*+}(1S, \frac{1}{2}^+)\gamma$ are tiny. For the $\Sigma_c(1P)$ states, we note that some radiative decay widths larger than 100 keV, such as $\Sigma_{c0}^0(1P, \frac{1}{2}^-) \rightarrow \Sigma_c^0(1S, \frac{1}{2}^+)\gamma$, $\Sigma_{c1}^0(1P, \frac{1}{2}^-) \rightarrow \Sigma_c^0(1S, \frac{1}{2}^+)\gamma$, and so on. But there are no large decay widths

for the $\Sigma_c^+(1P) \rightarrow \Sigma_c^+(1S, \frac{1}{2}^+)\gamma$ and $\Sigma_c^+(1P) \rightarrow \Sigma_c^{*+}(1S, \frac{3}{2}^+)\gamma$ decays. According to Table III, we suggest looking for the $\Sigma_c^0(1S, \frac{1}{2}^+)\gamma$, $\Sigma_c^{*0}(1S, \frac{3}{2}^+)\gamma$, $\Lambda_c^+(1S, \frac{1}{2}^+)\gamma$, $\Sigma_c^{*+}(1S, \frac{1}{2}^+)\gamma$, and $\Sigma_c^{*++}(1S, \frac{3}{2}^+)\gamma$ modes of the $\Sigma_c(1P)$. For the the $\Sigma_c(1D)$ and $\Sigma_c(1F)$, we find large radiative decay widths from the $\Sigma_c^+(1S, \frac{1}{2}^+)\gamma$ and $\Sigma_c^{*+}(1S, \frac{3}{2}^+)\gamma$ channels. Finally, for the two $\Sigma_c(2S)$ states, the partial widths of the $\Lambda_c^+(1S, \frac{1}{2}^+)\gamma$ mode are calculated to be larger than 100 keV. In addition, the $\Sigma_c^{*+}(1S, \frac{1}{2}^+)\gamma$ and $\Sigma_c^{*++}(1S, \frac{3}{2}^+)\gamma$ modes are also significant for the discussed $\Sigma_c(2S)$ state.

In the following, we will discuss the radiative decays of the Ξ'_c states. Two typical single-charm baryons are $\Xi_c^{(\prime)0}(1S, \frac{1}{2}^+)$ and $\Xi_c^{(\prime)+}(1S, \frac{1}{2}^+)$, where these two states have been observed in their radiative decays [17]. In Sec. III A, we point out that the coupling between the Ξ_c^0 state and $\Xi_c^0\gamma$ is forbidden if we employ strict SU(3) flavor symmetry. The conclusion remains the same if we reverse the initial and final single-charm baryons in the above transition. But it is obviously in conflict with the experimental data [17]. In Sec. III A, we consider the mass differences of $m_d - m_s$ to obtain small decay widths. In this subsection, we use the same approach to obtain the decay width of $\Xi_c^{(\prime)0}(1S, \frac{1}{2}^+) \rightarrow \Xi_c^0(1S, \frac{1}{2}^+)\gamma$ at 0.3 keV. We propose to measure the width of the $\Xi_c^{(\prime)0}(1S, \frac{1}{2}^+)$ in high precision experiments, which could test the SU(3) flavor symmetry and further unravel the structure of the single-charm baryon. In addition, the widths of the $\Xi_c^{(\prime)+}(1S, \frac{1}{2}^+)$ and $\Xi_c^{*+}(1S, \frac{3}{2}^+)$ decays into $\Xi_c^+(1S, \frac{1}{2}^+)\gamma$ are 14.9 and 52.7 keV, respectively. For the $\Xi'_c(1P)$ states, we find some partial widths that are larger than 100 keV corresponding to the $\Xi_c^{(\prime)0}(1S, \frac{1}{2}^+)\gamma$ and $\Xi_c^{(\prime)0}(1S, \frac{3}{2}^+)\gamma$ channels. So far, there are several good $\Xi'_c(1P)$ candidates have been observed in experiment, i.e., the $\Xi_c(2880)$, $\Xi_c(2923)$, $\Xi_c(2939)$, and $\Xi_c(2965)$ [67, 68]. In previous experiments, these states have been studied by surveying their strong decays. In fact, the search for these states is also interesting using different approaches such as their radiative decays with $\Xi_c^{(\prime)0}(1S, \frac{1}{2}^+)\gamma$ and $\Xi_c^{(\prime)0}(1S, \frac{3}{2}^+)\gamma$ channels. In this work, we do not find the radiative decay widths of the discussed $\Xi'_c(1D)$ and $\Xi'_c(1F)$ states that are larger than 50 keV as indicated in Table III. For the two $\Xi'_c(2S)$ states, the decay widths of their $\Xi_c^+(1S, \frac{1}{2}^+)\gamma$ modes are much more larger than other radiative decay channels.

For the $\Omega_c^{*0}(1S, \frac{3}{2}^+)$ state, the dominant radiative decay channel is $\Omega_c^0(1S, \frac{1}{2}^+)\gamma$, which has been observed in experiments [18, 19]. In 2017, the LHCb Collaboration [69] observed the $\Omega_c(3000)$, $\Omega_c(3050)$, $\Omega_c(3065)$, $\Omega_c(3090)$, and $\Omega_c(3119)$ from the pp collisions. According to the theoretical mass spectra and decay widths [42, 70–82], they could be considered as $\Omega_c(1P)$ or $\Omega_c(2S)$ candidates. In 2023, these states were confirmed in the same productions [83]. In addition, except for $\Omega_c(3119)$, the remaining four states were observed in e^+e^- collisions by the Belle Collaboration [84] and in $\Omega_b^- \rightarrow \Omega_c^0(?)\pi^- \rightarrow \Xi_c^+ K^- \pi^-$ by the LHCb Collaboration [85]. However, their J^P quantum numbers are still unknown. According to Table III, the radiative decay channels $\Omega_c^0(1S, \frac{1}{2}^+)\gamma$

TABLE II: The radiative decay widths (in units of keV) of single-charm baryons in the $\bar{3}_f$ representation decaying into the $\Lambda_c(1S)/\Sigma_c(1S)/\Xi_c^{(\prime)}(1S)\gamma$.

Process	Our	Ref. [41]	Ref. [34]	Process	Our	Ref. [41]	Ref. [34]	Expt. [20]
$\Lambda_c^+(1P, \frac{1}{2}^-) \rightarrow \Lambda_c^+(1S, \frac{1}{2}^+)\gamma$	0.1	0.26	0.1	$\Xi_c^0(1P, \frac{1}{2}^-) \rightarrow \Xi_c^0(1S, \frac{1}{2}^+)\gamma$	217.5	263	202.5	800 ± 320
$\Lambda_c^+(1P, \frac{1}{2}^-) \rightarrow \Sigma_c^+(1S, \frac{1}{2}^+)\gamma$	0.3	0.45	1.0	$\Xi_c^0(1P, \frac{1}{2}^-) \rightarrow \Xi_c^{*0}(1S, \frac{1}{2}^+)\gamma$	0.0	0.0	0.0	...
$\Lambda_c^+(1P, \frac{1}{2}^-) \rightarrow \Sigma_c^{*+}(1S, \frac{3}{2}^+)\gamma$	0.0	0.05	0.0	$\Xi_c^0(1P, \frac{1}{2}^-) \rightarrow \Xi_c^{*0}(1S, \frac{3}{2}^+)\gamma$	0.0	0.0	0.0	...
$\Lambda_c^+(1P, \frac{3}{2}^-) \rightarrow \Lambda_c^+(1S, \frac{1}{2}^+)\gamma$	0.8	0.30	0.7	$\Xi_c^0(1P, \frac{3}{2}^-) \rightarrow \Xi_c^0(1S, \frac{1}{2}^+)\gamma$	243.1	292	292.6	$320 \pm 45_{-80}^{+45}$
$\Lambda_c^+(1P, \frac{3}{2}^-) \rightarrow \Sigma_c^+(1S, \frac{1}{2}^+)\gamma$	0.9	1.17	2.5	$\Xi_c^0(1P, \frac{3}{2}^-) \rightarrow \Xi_c^{*0}(1S, \frac{1}{2}^+)\gamma$	0.0	0.0	0.1	...
$\Lambda_c^+(1P, \frac{3}{2}^-) \rightarrow \Sigma_c^{*+}(1S, \frac{3}{2}^+)\gamma$	0.2	0.26	0.2	$\Xi_c^0(1P, \frac{3}{2}^-) \rightarrow \Xi_c^{*0}(1S, \frac{3}{2}^+)\gamma$	0.0	0.0	0.0	...
				$\Xi_c^+(1P, \frac{1}{2}^-) \rightarrow \Xi_c^+(1S, \frac{1}{2}^+)\gamma$	1.7	4.65	7.4	< 350
				$\Xi_c^+(1P, \frac{1}{2}^-) \rightarrow \Xi_c^{\prime+}(1S, \frac{1}{2}^+)\gamma$	1.2	1.43	1.3	...
				$\Xi_c^+(1P, \frac{1}{2}^-) \rightarrow \Xi_c^{*+}(1S, \frac{3}{2}^+)\gamma$	0.5	0.44	0.1	...
				$\Xi_c^+(1P, \frac{3}{2}^-) \rightarrow \Xi_c^+(1S, \frac{1}{2}^+)\gamma$	1.0	2.8	4.8	< 80
				$\Xi_c^+(1P, \frac{3}{2}^-) \rightarrow \Xi_c^{\prime+}(1S, \frac{1}{2}^+)\gamma$	2.1	2.32	2.9	...
				$\Xi_c^+(1P, \frac{3}{2}^-) \rightarrow \Xi_c^{*+}(1S, \frac{3}{2}^+)\gamma$	1.2	0.99	0.3	...

Process	Our	Process	Our	Process	Our
$\Lambda_c^+(1D, \frac{3}{2}^+) \rightarrow \Lambda_c^+(1S, \frac{1}{2}^+)\gamma$	41.3	$\Xi_c^0(1D, \frac{3}{2}^+) \rightarrow \Xi_c^0(1S, \frac{1}{2}^+)\gamma$	17.8	$\Xi_c^+(1D, \frac{3}{2}^+) \rightarrow \Xi_c^+(1S, \frac{1}{2}^+)\gamma$	28.2
$\Lambda_c^+(1D, \frac{3}{2}^+) \rightarrow \Sigma_c^+(1S, \frac{1}{2}^+)\gamma$	1.4	$\Xi_c^0(1D, \frac{3}{2}^+) \rightarrow \Xi_c^{*0}(1S, \frac{1}{2}^+)\gamma$	0.0	$\Xi_c^+(1D, \frac{3}{2}^+) \rightarrow \Xi_c^{\prime+}(1S, \frac{1}{2}^+)\gamma$	1.3
$\Lambda_c^+(1D, \frac{3}{2}^+) \rightarrow \Sigma_c^{*+}(1S, \frac{3}{2}^+)\gamma$	1.3	$\Xi_c^0(1D, \frac{3}{2}^+) \rightarrow \Xi_c^{*0}(1S, \frac{3}{2}^+)\gamma$	0.0	$\Xi_c^+(1D, \frac{3}{2}^+) \rightarrow \Xi_c^{*+}(1S, \frac{3}{2}^+)\gamma$	1.6
$\Lambda_c^+(1D, \frac{5}{2}^+) \rightarrow \Lambda_c^+(1S, \frac{1}{2}^+)\gamma$	42.8	$\Xi_c^0(1D, \frac{5}{2}^+) \rightarrow \Xi_c^0(1S, \frac{1}{2}^+)\gamma$	21.4	$\Xi_c^+(1D, \frac{5}{2}^+) \rightarrow \Xi_c^+(1S, \frac{1}{2}^+)\gamma$	27.1
$\Lambda_c^+(1D, \frac{5}{2}^+) \rightarrow \Sigma_c^+(1S, \frac{1}{2}^+)\gamma$	1.9	$\Xi_c^0(1D, \frac{5}{2}^+) \rightarrow \Xi_c^{*0}(1S, \frac{1}{2}^+)\gamma$	0.0	$\Xi_c^+(1D, \frac{5}{2}^+) \rightarrow \Xi_c^{\prime+}(1S, \frac{1}{2}^+)\gamma$	1.6
$\Lambda_c^+(1D, \frac{5}{2}^+) \rightarrow \Sigma_c^{*+}(1S, \frac{3}{2}^+)\gamma$	2.0	$\Xi_c^0(1D, \frac{5}{2}^+) \rightarrow \Xi_c^{*0}(1S, \frac{3}{2}^+)\gamma$	0.0	$\Xi_c^+(1D, \frac{5}{2}^+) \rightarrow \Xi_c^{*+}(1S, \frac{3}{2}^+)\gamma$	2.0
$\Lambda_c^+(1F, \frac{3}{2}^-) \rightarrow \Lambda_c^+(1S, \frac{1}{2}^+)\gamma$	4.6	$\Xi_c^0(1F, \frac{3}{2}^-) \rightarrow \Xi_c^0(1S, \frac{1}{2}^+)\gamma$	28.4	$\Xi_c^+(1F, \frac{3}{2}^-) \rightarrow \Xi_c^+(1S, \frac{1}{2}^+)\gamma$	0.1
$\Lambda_c^+(1F, \frac{3}{2}^-) \rightarrow \Sigma_c^+(1S, \frac{1}{2}^+)\gamma$	0.9	$\Xi_c^0(1F, \frac{3}{2}^-) \rightarrow \Xi_c^{*0}(1S, \frac{1}{2}^+)\gamma$	0.0	$\Xi_c^+(1F, \frac{3}{2}^-) \rightarrow \Xi_c^{\prime+}(1S, \frac{1}{2}^+)\gamma$	0.6
$\Lambda_c^+(1F, \frac{3}{2}^-) \rightarrow \Sigma_c^{*+}(1S, \frac{3}{2}^+)\gamma$	1.2	$\Xi_c^0(1F, \frac{3}{2}^-) \rightarrow \Xi_c^{*0}(1S, \frac{3}{2}^+)\gamma$	0.0	$\Xi_c^+(1F, \frac{3}{2}^-) \rightarrow \Xi_c^{*+}(1S, \frac{3}{2}^+)\gamma$	0.9
$\Lambda_c^+(1F, \frac{7}{2}^-) \rightarrow \Lambda_c^+(1S, \frac{1}{2}^+)\gamma$	4.8	$\Xi_c^0(1F, \frac{7}{2}^-) \rightarrow \Xi_c^0(1S, \frac{1}{2}^+)\gamma$	26.9	$\Xi_c^+(1F, \frac{7}{2}^-) \rightarrow \Xi_c^+(1S, \frac{1}{2}^+)\gamma$	0.1
$\Lambda_c^+(1F, \frac{7}{2}^-) \rightarrow \Sigma_c^+(1S, \frac{1}{2}^+)\gamma$	0.9	$\Xi_c^0(1F, \frac{7}{2}^-) \rightarrow \Xi_c^{*0}(1S, \frac{1}{2}^+)\gamma$	0.0	$\Xi_c^+(1F, \frac{7}{2}^-) \rightarrow \Xi_c^{\prime+}(1S, \frac{1}{2}^+)\gamma$	0.6
$\Lambda_c^+(1F, \frac{7}{2}^-) \rightarrow \Sigma_c^{*+}(1S, \frac{3}{2}^+)\gamma$	1.2	$\Xi_c^0(1F, \frac{7}{2}^-) \rightarrow \Xi_c^{*0}(1S, \frac{3}{2}^+)\gamma$	0.0	$\Xi_c^+(1F, \frac{7}{2}^-) \rightarrow \Xi_c^{*+}(1S, \frac{3}{2}^+)\gamma$	0.9
$\Lambda_c^+(2S, \frac{1}{2}^+) \rightarrow \Lambda_c^+(1S, \frac{1}{2}^+)\gamma$	0.0	$\Xi_c^0(2S, \frac{1}{2}^+) \rightarrow \Xi_c^0(1S, \frac{1}{2}^+)\gamma$	0.0	$\Xi_c^+(2S, \frac{1}{2}^+) \rightarrow \Xi_c^+(1S, \frac{1}{2}^+)\gamma$	0.0
$\Lambda_c^+(2S, \frac{1}{2}^+) \rightarrow \Sigma_c^+(1S, \frac{1}{2}^+)\gamma$	0.0	$\Xi_c^0(2S, \frac{1}{2}^+) \rightarrow \Xi_c^{*0}(1S, \frac{1}{2}^+)\gamma$	0.1	$\Xi_c^+(2S, \frac{1}{2}^+) \rightarrow \Xi_c^{\prime+}(1S, \frac{1}{2}^+)\gamma$	0.9
$\Lambda_c^+(2S, \frac{1}{2}^+) \rightarrow \Sigma_c^{*+}(1S, \frac{3}{2}^+)\gamma$	3.2	$\Xi_c^0(2S, \frac{1}{2}^+) \rightarrow \Xi_c^{*0}(1S, \frac{3}{2}^+)\gamma$	0.0	$\Xi_c^+(2S, \frac{1}{2}^+) \rightarrow \Xi_c^{*+}(1S, \frac{3}{2}^+)\gamma$	1.4

and $\Omega_c^{*0}(1S, \frac{3}{2}^+)\gamma$ of the $\Omega_c(1P)$ have larger widths. This gives us a new approach to study these states. We propose to study the $\Omega_c(1P)$ states in the $\Omega_c^0(1S, \frac{1}{2}^+)\gamma$ and $\Omega_c^{*0}(1S, \frac{3}{2}^+)\gamma$ channels. However, for the $\Omega_c(1D)$, $\Omega_c(1F)$, and $\Omega_c(2S)$, both partial widths of the $\Omega_c^0(1S, \frac{1}{2}^+)\gamma$ and $\Omega_c^{*0}(1S, \frac{3}{2}^+)\gamma$ channels are not obvious. Although observations of the higher excited states $\Omega_c(3188)$ and $\Omega_c(3327)$ help us to construct the $\Omega_c(2S)$ and $\Omega_c(1D)$ spectroscopy [48, 69, 83, 84, 86–89], the search for the $\Omega_c(1D)$, $\Omega_c(1F)$, and $\Omega_c(2S)$ in $\Omega_c^0(1S, \frac{1}{2}^+)\gamma$ and $\Omega_c^{*0}(1S, \frac{3}{2}^+)\gamma$ processes is really difficult in the expected future.

IV. SUMMARY

At the beginning of the 21st century, the situation of observing single-charm baryons has changed, as more and more single-charm baryons have been reported in various experi-

ments such as Belle and LHCb. It can be reflected by checking the presently collected single-charm baryons in the PDG [16]. Although the radiative decays of single-charm baryons have not been extensively reported compared to these observed strong and weak decay modes, the radiative decay of single-charm baryons is one aspect of the whole decay behavior of them that should be paid more attention. In particular, in the face of the high-precision era of hadron spectroscopy, we have reason to believe that more radiative decays of single-charm baryons will become experimentally accessible. With the promotion of experimental precision, we need to increase theoretical precision.

In this work, we revisit the radiative decays of single-charm baryons. In contrast to the treatment in the previous work [46], we adopt the numerical spatial wave function for the single-charm baryon, which can be obtained by the concrete potential model and with the approach the GEM [47]. This treatment can meet the requirements of high-precision hadron

TABLE III: The radiative decay widths (in units of keV) of single-charm baryons in the 6_f representation decaying into the $\Lambda_c(1S)/\Sigma_c(1S)/\Xi_c^{(\prime)}(1S)/\Omega_c(1S)\gamma$.

Process	Our	Ref. [41]	Ref. [34]	Ref. [35]	Process	Our	Ref. [41]	Ref. [34]	Ref. [35]
$\Sigma_c^{*0}(1S, \frac{3}{2}^+) \rightarrow \Sigma_c^0(1S, \frac{1}{2}^+) \gamma$	1.3	3.43	1.8	1.378	$\Xi_c^{*0}(1S, \frac{1}{2}^+) \rightarrow \Xi_c^0(1S, \frac{1}{2}^+) \gamma$	0.3	0.0	0.4	0.342
$\Sigma_c^+(1S, \frac{1}{2}^+) \rightarrow \Lambda_c^+(1S, \frac{1}{2}^+) \gamma$	59.2	80.6	87.2	93.5	$\Xi_c^{*0}(1S, \frac{3}{2}^+) \rightarrow \Xi_c^0(1S, \frac{1}{2}^+) \gamma$	1.1	0.0	1.6	1.322
$\Sigma_c^{*+}(1S, \frac{3}{2}^+) \rightarrow \Lambda_c^+(1S, \frac{1}{2}^+) \gamma$	132.8	373	199.4	231	$\Xi_c^{*0}(1S, \frac{3}{2}^+) \rightarrow \Xi_c^0(1S, \frac{1}{2}^+) \gamma$	1.0	3.03	1.4	1.262
$\Sigma_c^{*+}(1S, \frac{3}{2}^+) \rightarrow \Sigma_c^+(1S, \frac{1}{2}^+) \gamma$	0.0	0.004	0.0	0.00067	$\Xi_c^{*+}(1S, \frac{1}{2}^+) \rightarrow \Xi_c^+(1S, \frac{1}{2}^+) \gamma$	14.9	42.3	20.6	21.38
$\Sigma_c^{*++}(1S, \frac{3}{2}^+) \rightarrow \Sigma_c^{++}(1S, \frac{1}{2}^+) \gamma$	1.7	3.94	2.1	1.483	$\Xi_c^{*+}(1S, \frac{3}{2}^+) \rightarrow \Xi_c^+(1S, \frac{1}{2}^+) \gamma$	52.7	139	74.2	81.9
					$\Xi_c^{*+}(1S, \frac{3}{2}^+) \rightarrow \Xi_c^+(1S, \frac{1}{2}^+) \gamma$	0.1	0.004	0.1	0.029
					$\Omega_c^{*0}(1S, \frac{3}{2}^+) \rightarrow \Omega_c^0(1S, \frac{1}{2}^+) \gamma$	0.9	0.89	1.0	1.14

	$\Sigma_c^0(1S, \frac{1}{2}^+) \gamma$	$\Sigma_c^{*0}(1S, \frac{3}{2}^+) \gamma$	$\Lambda_c^+(1S, \frac{1}{2}^+) \gamma$	$\Sigma_c^+(1S, \frac{1}{2}^+) \gamma$	$\Sigma_c^{*+}(1S, \frac{3}{2}^+) \gamma$	$\Sigma_c^{++}(1S, \frac{1}{2}^+) \gamma$	$\Sigma_c^{*++}(1S, \frac{3}{2}^+) \gamma$
$\Sigma_{c0}^{0,++}(1P, \frac{1}{2}^-)$	137.8	183.0	0.0	3.3	2.7	236.2	281.6
$\Sigma_{c1}^{0,++}(1P, \frac{1}{2}^-)$	202.7	68.4	84.5	1.5	0.9	279.0	93.4
$\Sigma_{c1}^{0,++}(1P, \frac{3}{2}^-)$	59.3	209.2	95.8	1.9	1.8	101.1	291.4
$\Sigma_{c2}^{0,++}(1P, \frac{3}{2}^-)$	158.8	25.5	49.9	1.9	0.7	133.6	26.8
$\Sigma_{c2}^{0,++}(1P, \frac{5}{2}^-)$	1.5	148.2	53.5	1.1	0.7	11.1	148.9
$\Sigma_{c1}^{0,++}(1D, \frac{1}{2}^+)$	0.8	76.6	11.0	0.1	56.0	2.5	562.5
$\Sigma_{c1}^{0,++}(1D, \frac{3}{2}^+)$	46.5	42.0	11.1	32.3	29.3	330.8	299.2
$\Sigma_{c2}^{0,++}(1D, \frac{3}{2}^+)$	26.0	24.6	29.8	22.9	20.6	214.6	195.7
$\Sigma_{c2}^{0,++}(1D, \frac{5}{2}^+)$	13.7	39.9	30.0	10.0	31.8	99.9	308.8
$\Sigma_{c3}^{0,++}(1D, \frac{5}{2}^+)$	13.6	4.9	14.6	19.7	5.3	156.6	45.7
$\Sigma_{c3}^{0,++}(1D, \frac{7}{2}^+)$	1.1	19.5	14.6	0.1	21.5	3.2	186.8
$\Sigma_{c2}^{0,++}(1F, \frac{3}{2}^-)$	0.2	63.5	3.7	0.1	7.3	1.2	178.3
$\Sigma_{c2}^{0,++}(1F, \frac{5}{2}^-)$	32.9	28.1	3.6	3.8	3.4	92.6	80.7
$\Sigma_{c3}^{0,++}(1F, \frac{5}{2}^-)$	17.3	22.8	8.2	1.7	2.4	45.7	62.1
$\Sigma_{c3}^{0,++}(1F, \frac{7}{2}^-)$	9.7	29.8	8.0	1.1	3.3	26.8	82.8
$\Sigma_{c4}^{0,++}(1F, \frac{7}{2}^-)$	14.1	5.3	3.8	1.0	0.5	32.7	13.4
$\Sigma_{c4}^{0,++}(1F, \frac{9}{2}^-)$	0.2	18.9	3.8	0.1	1.7	1.1	48.5
$\Sigma_c^{0,++}(2S, \frac{1}{2}^+)$	14.6	0.4	117.8	3.3	0.8	55.6	5.8
$\Sigma_c^{*0,++}(2S, \frac{3}{2}^+)$	10.8	11.5	151.2	0.7	3.5	24.3	50.9

	$\Xi_c^0(1S, \frac{1}{2}^+) \gamma$	$\Xi_c^{*0}(1S, \frac{1}{2}^+) \gamma$	$\Xi_c^{*0}(1S, \frac{3}{2}^+) \gamma$	$\Xi_c^+(1S, \frac{1}{2}^+) \gamma$	$\Xi_c^{*+}(1S, \frac{1}{2}^+) \gamma$	$\Xi_c^{*+}(1S, \frac{3}{2}^+) \gamma$	$\Omega_c^0(1S, \frac{1}{2}^+) \gamma$	$\Omega_c^{*0}(1S, \frac{3}{2}^+) \gamma$	
$\Xi_{c0}^{0,+}(1P, \frac{1}{2}^-)$	0.0	109.0	150.1	0.0	1.2	0.6	$\Omega_{c0}^0(1P, \frac{1}{2}^-)$	83.7	110.2
$\Xi_{c1}^{0,+}(1P, \frac{1}{2}^-)$	0.5	172.8	59.7	36.3	0.0	1.0	$\Omega_{c1}^0(1P, \frac{1}{2}^-)$	143.6	46.9
$\Xi_{c1}^{0,+}(1P, \frac{3}{2}^-)$	0.6	50.1	187.3	44.9	1.6	0.3	$\Omega_{c1}^0(1P, \frac{3}{2}^-)$	41.8	154.3
$\Xi_{c2}^{0,+}(1P, \frac{3}{2}^-)$	0.3	165.4	26.9	24.3	9.6	2.2	$\Omega_{c2}^0(1P, \frac{3}{2}^-)$	168.3	26.2
$\Xi_{c2}^{0,+}(1P, \frac{5}{2}^-)$	0.4	0.7	156.8	27.1	1.7	5.1	$\Omega_{c2}^0(1P, \frac{5}{2}^-)$	0.2	155.1
$\Xi_{c1}^{0,+}(1D, \frac{1}{2}^+)$	0.0	0.4	32.4	4.4	0.1	38.1	$\Omega_{c1}^0(1D, \frac{1}{2}^+)$	0.2	11.4
$\Xi_{c1}^{0,+}(1D, \frac{3}{2}^+)$	0.0	20.9	18.4	4.6	19.8	19.5	$\Omega_{c1}^0(1D, \frac{3}{2}^+)$	8.5	6.9
$\Xi_{c2}^{0,+}(1D, \frac{3}{2}^+)$	0.1	11.6	10.7	12.5	14.7	14.4	$\Omega_{c2}^0(1D, \frac{3}{2}^+)$	4.5	3.9
$\Xi_{c2}^{0,+}(1D, \frac{5}{2}^+)$	0.1	6.5	18.2	12.9	6.1	21.3	$\Omega_{c2}^0(1D, \frac{5}{2}^+)$	2.8	7.2
$\Xi_{c3}^{0,+}(1D, \frac{5}{2}^+)$	0.0	5.9	2.3	6.5	12.4	3.8	$\Omega_{c3}^0(1D, \frac{5}{2}^+)$	2.1	0.9
$\Xi_{c3}^{0,+}(1D, \frac{7}{2}^+)$	0.0	0.6	9.3	6.5	0.1	14.0	$\Omega_{c3}^0(1D, \frac{7}{2}^+)$	0.4	3.9
$\Xi_{c2}^{0,+}(1F, \frac{3}{2}^-)$	0.0	0.1	39.3	1.3	0.1	0.2	$\Omega_{c2}^0(1F, \frac{3}{2}^-)$	0.0	24.5
$\Xi_{c2}^{0,+}(1F, \frac{5}{2}^-)$	0.0	20.5	17.2	1.3	0.0	0.1	$\Omega_{c2}^0(1F, \frac{5}{2}^-)$	13.0	10.7
$\Xi_{c3}^{0,+}(1F, \frac{5}{2}^-)$	0.0	12.0	15.5	3.0	0.1	0.1	$\Omega_{c3}^0(1F, \frac{5}{2}^-)$	8.5	10.8
$\Xi_{c3}^{0,+}(1F, \frac{7}{2}^-)$	0.0	6.5	20.0	3.0	0.1	0.1	$\Omega_{c3}^0(1F, \frac{7}{2}^-)$	4.5	13.8
$\Xi_{c4}^{0,+}(1F, \frac{7}{2}^-)$	0.0	11.7	4.2	1.4	0.3	0.1	$\Omega_{c4}^0(1F, \frac{7}{2}^-)$	9.9	3.5
$\Xi_{c4}^{0,+}(1F, \frac{9}{2}^-)$	0.0	0.1	15.1	1.4	0.1	0.2	$\Omega_{c4}^0(1F, \frac{9}{2}^-)$	0.0	12.3
$\Xi_c^{0,+}(2S, \frac{1}{2}^+)$	1.2	7.4	0.0	46.9	6.2	1.1	$\Omega_c^0(2S, \frac{1}{2}^+)$	3.0	0.2
$\Xi_c^{*0,+}(2S, \frac{3}{2}^+)$	1.3	7.6	5.4	74.9	1.4	6.0	$\Omega_c^{*0}(2S, \frac{3}{2}^+)$	5.4	1.9

spectroscopy. We also make a comparison with the current experimental data [20] and the theoretical results from other groups [34, 35, 41], as summarized in the last section.

With the running of Belle II [49, 50] and Run-3 and Run-4 of LHCb [51, 52], we can expect more observations of single-charm baryons. This information on the radiative decay of single-charm baryons will stimulate our experimental colleagues to focus on exploring the spectroscopy of single-charm baryons.

Acknowledgments

This work is supported by the National Natural Science Foundation of China under Grants No. 12335001 and

No. 12247101, National Key Research and Development Program of China under Contract No. 2020YFA0406400, the 111 Project under Grant No. B20063, the fundamental Research Funds for the Central Universities, and the project for top-notch innovative talents of Gansu province.

Appendix A: Some additional radiative decay widths

In Tables IV-VII, we also list the calculated results of other radiative decay widths of single-charm baryons. The final states of these discussed radiative decays are involved in radial or orbital excited states of single-charm baryons. This information is left to the readers who are interested in exploring these allowed radiative decays.

-
- [1] X. Liu, An overview of XYZ new particles, *Chin. Sci. Bull.* **59**, 3815–3830 (2014).
- [2] H. Y. Cheng, Charmed baryons circa 2015, *Front. Phys. (Beijing)* **10**, 101406 (2015).
- [3] H. X. Chen, W. Chen, X. Liu, Y. R. Liu, and S. L. Zhu, A review of the open charm and open bottom systems, *Rept. Prog. Phys.* **80**, 076201 (2017).
- [4] H. X. Chen, W. Chen, X. Liu, and S. L. Zhu, The hidden-charm pentaquark and tetraquark states, *Phys. Rept.* **639**, 1–121 (2016).
- [5] E. Klempt and J. M. Richard, Baryon spectroscopy, *Rev. Mod. Phys.* **82**, 1095–1153 (2010).
- [6] F. K. Guo, C. Hanhart, U. G. Meißner, Q. Wang, Q. Zhao, and B. S. Zou, Hadronic molecules, *Rev. Mod. Phys.* **90**, 015004 (2018), [Erratum: *Rev. Mod. Phys.* **94**, 029901 (2022)].
- [7] N. Brambilla, S. Eidelman, C. Hanhart, A. Nefediev, C. P. Shen, C. E. Thomas, A. Vairo, and C. Z. Yuan, The XYZ states: experimental and theoretical status and perspectives, *Phys. Rept.* **873**, 1–154 (2020).
- [8] Y. R. Liu, H. X. Chen, W. Chen, X. Liu, and S. L. Zhu, Pentaquark and tetraquark states, *Prog. Part. Nucl. Phys.* **107**, 237–320 (2019).
- [9] H. Y. Cheng, Charmed baryon physics circa 2021, *Chin. J. Phys.* **78**, 324–362 (2022).
- [10] L. Meng, B. Wang, G. J. Wang, and S. L. Zhu, Chiral perturbation theory for heavy hadrons and chiral effective field theory for heavy hadronic molecules, *Phys. Rept.* **1019**, 1–149 (2023).
- [11] H. X. Chen, W. Chen, X. Liu, Y. R. Liu, and S. L. Zhu, An updated review of the new hadron states, *Rept. Prog. Phys.* **86**, 026201 (2023).
- [12] X. Chu (BES III Collaboration), Hadron spectroscopy at BES III, *PoS HQL2016*, 028 (2017).
- [13] J. Wang (LHCb Collaboration), Heavy flavour and exotic production at LHCb, *PoS ICHEP2022*, 487 (2022).
- [14] J. Xu (LHCb Collaboration), LHCb results in charm baryons, *Nucl. Part. Phys. Proc.* **318-323**, 56–60 (2022).
- [15] Y. Onuki (Belle-II Collaboration), Belle II status and prospect, *Nucl. Part. Phys. Proc.* **318-323**, 78–84 (2022).
- [16] R. L. Workman *et al.* (Particle Data Group), Review of Particle Physics, *PTEP* **2022**, 083C01 (2022).
- [17] C. P. Jessop *et al.* (CLEO Collaboration), Observation of two narrow states decaying into $\Xi_c^+\gamma$ and $\Xi_c^0\gamma$, *Phys. Rev. Lett.* **82**, 492–496 (1999).
- [18] B. Aubert *et al.* (BaBar Collaboration), Observation of an excited charm baryon Ω_c^* decaying to $\Omega_c^0\gamma$, *Phys. Rev. Lett.* **97**, 232001 (2006).
- [19] E. Solovieva *et al.*, Study of Ω_c^0 and Ω_c^{*0} baryons at Belle, *Phys. Lett. B* **672**, 1–5 (2009).
- [20] J. Yelton *et al.* (Belle Collaboration), Study of electromagnetic decays of orbitally excited Ξ_c baryons, *Phys. Rev. D* **102**, 071103 (2020).
- [21] T. M. Aliev, K. Azizi, and A. Ozpineci, Radiative Decays of the Heavy Flavored Baryons in Light Cone QCD Sum Rules, *Phys. Rev. D* **79**, 056005 (2009).
- [22] T. M. Aliev, K. Azizi, and H. Sundu, Radiative $\Omega_c^* \rightarrow \Omega_c\gamma$ and $\Xi_c^* \rightarrow \Xi_c\gamma$ transitions in light cone QCD, *Eur. Phys. J. C* **75**, 14 (2015).
- [23] T. M. Aliev, T. Barakat, and M. Savcı, Analysis of the radiative decays $\Sigma_c \rightarrow \Lambda_c\gamma$ and $\Xi_c' \rightarrow \Xi_c\gamma$ in light cone sum rules, *Phys. Rev. D* **93**, 056007 (2016).
- [24] Z. G. Wang, Analysis of the vertexes $\Omega_c^*\Omega_c\phi$ and radiative decays $\Omega_c^* \rightarrow \Omega_c\gamma$, *Phys. Rev. D* **81**, 036002 (2010).
- [25] Z. G. Wang, Analysis of the vertexes $\Xi_c^*\Xi_c'V$, $\Sigma_c^*\Sigma_c V$ and radiative decays $\Xi_c^* \rightarrow \Xi_c'\gamma$, $\Sigma_c^* \rightarrow \Sigma_c\gamma$, *Eur. Phys. J. A* **44**, 105–117 (2010).
- [26] S. L. Zhu and Y. B. Dai, Radiative decays of heavy hadrons from light cone QCD sum rules in the leading order of HQET, *Phys. Rev. D* **59**, 114015 (1999).
- [27] H. Y. Cheng, C. Y. Cheung, G. L. Lin, Y. C. Lin, T. M. Yan, and H. L. Yu, Chiral Lagrangians for radiative decays of heavy hadrons, *Phys. Rev. D* **47**, 1030–1042 (1993).
- [28] S. L. Zhu, Strong and electromagnetic decays of p -wave heavy baryons Λ_{c1} , Λ_{c1}^* , *Phys. Rev. D* **61**, 114019 (2000).
- [29] S. Tawfiq, J. G. Korner, and P. J. O'Donnell, Electromagnetic transitions of heavy baryons in the $SU(2N_f) \otimes O(3)$ symmetry, *Phys. Rev. D* **63**, 034005 (2001).
- [30] H. S. Li, L. Meng, Z. W. Liu, and S. L. Zhu, Radiative decays of the doubly charmed baryons in chiral perturbation theory, *Phys. Lett. B* **777**, 169–176 (2018).
- [31] N. Jiang, X. L. Chen, and S. L. Zhu, Electromagnetic decays of the charmed and bottom baryons in chiral perturbation theory, *Phys. Rev. D* **92**, 054017 (2015).
- [32] G. J. Wang, L. Meng, and S. L. Zhu, Radiative decays of the singly heavy baryons in chiral perturbation theory, *Phys. Rev. D* **99**, 034021 (2019).
- [33] K. Gandhi, Z. Shah, and A. K. Rai, Spectrum of nonstrange

TABLE IV: Radiative decay widths of 3_f single-charm baryon decaying into radial or orbital excited states.

	$\Lambda_c^+/\Xi_c^{0,+}(1P, \frac{1}{2}^-)\gamma$			$\Lambda_c^+/\Xi_c^{0,+}(1P, \frac{3}{2}^-)\gamma$			$\Lambda_c^+/\Xi_c^{0,+}(2S, \frac{1}{2}^+)\gamma$		
	Λ_c^+	Ξ_c^0	Ξ_c^+	Λ_c^+	Ξ_c^0	Ξ_c^+	Λ_c^+	Ξ_c^0	Ξ_c^+
$\Lambda_c^+/\Xi_c^{0,+}(2S, \frac{1}{2}^+)$	0.3	45.9	0.0	0.2	68.1	0.1
$\Lambda_c^+/\Xi_c^{0,+}(1D, \frac{3}{2}^+)$	0.3	270.4	1.2	0.1	46.0	0.4	0.1	0.0	0.0
$\Lambda_c^+/\Xi_c^{0,+}(1D, \frac{5}{2}^+)$	0.3	0.6	0.1	1.1	298.8	0.6	0.3	0.1	0.1
$\Lambda_c^+/\Xi_c^{0,+}(1F, \frac{5}{2}^-)$	74.3	35.7	55.2	19.8	10.0	15.6	1.1	3.7	0.2
$\Lambda_c^+/\Xi_c^{0,+}(1F, \frac{7}{2}^-)$	0.7	0.7	0.2	81.5	48.4	61.7	1.2	3.9	0.3

	$\Lambda_c^+/\Xi_c^{0,+}(1D, \frac{3}{2}^+)\gamma$			$\Lambda_c^+/\Xi_c^{0,+}(1D, \frac{5}{2}^+)\gamma$			$\Sigma_c^+/\Xi_c^{0,+}(1P, \frac{1}{2}^-)\gamma$			$\Sigma_c^+/\Xi_c^{0,+}(1P, \frac{1}{2}^-)\gamma$		
	Λ_c^+	Ξ_c^0	Ξ_c^+	Λ_c^+	Ξ_c^0	Ξ_c^+	Σ_c^+	Ξ_c^0	Ξ_c^+	Σ_c^+	Ξ_c^0	Ξ_c^+
$\Lambda_c^+/\Xi_c^{0,+}(2S, \frac{1}{2}^+)$	0.0	0.0	...	0.0	0.0
$\Lambda_c^+/\Xi_c^{0,+}(1D, \frac{3}{2}^+)$	0.0	0.0	0.1	0.1	0.0	0.4
$\Lambda_c^+/\Xi_c^{0,+}(1D, \frac{5}{2}^+)$	0.0	0.0	0.0	0.0	0.0	0.2	0.0	0.0	0.2
$\Lambda_c^+/\Xi_c^{0,+}(1F, \frac{5}{2}^-)$	0.5	398.6	1.7	0.0	26.6	0.3	0.3	0.0	0.5	0.8	0.0	1.2
$\Lambda_c^+/\Xi_c^{0,+}(1F, \frac{7}{2}^-)$	0.1	0.3	0.1	1.1	354.3	0.6	0.3	0.0	0.5	0.2	0.0	0.3

	$\Sigma_c^+/\Xi_c^{0,+}(1P, \frac{3}{2}^-)\gamma$			$\Sigma_c^+/\Xi_c^{0,+}(1P, \frac{3}{2}^-)\gamma$			$\Sigma_c^+/\Xi_c^{0,+}(1P, \frac{5}{2}^-)\gamma$			$\Sigma_c^+/\Xi_c^{0,+}(2S, \frac{1}{2}^+)\gamma$		
	Σ_c^+	Ξ_c^0	Ξ_c^+	Σ_c^+	Ξ_c^0	Ξ_c^+	Σ_c^+	Ξ_c^0	Ξ_c^+	Σ_c^+	Ξ_c^0	Ξ_c^+
$\Lambda_c^+/\Xi_c^{0,+}(2S, \frac{1}{2}^+)$...	0.0	0.0	...	0.0	0.0	...	0.0	0.0
$\Lambda_c^+/\Xi_c^{0,+}(1D, \frac{3}{2}^+)$	0.0	0.0	0.1	0.1	0.0	0.5	0.0	0.0	0.0
$\Lambda_c^+/\Xi_c^{0,+}(1D, \frac{5}{2}^+)$	0.1	0.0	0.4	0.0	0.0	0.1	0.1	0.0	0.5
$\Lambda_c^+/\Xi_c^{0,+}(1F, \frac{5}{2}^-)$	0.3	0.0	0.5	1.5	0.0	2.1	0.3	0.0	0.5	0.0	0.0	0.0
$\Lambda_c^+/\Xi_c^{0,+}(1F, \frac{7}{2}^-)$	0.8	0.0	1.2	0.2	0.0	0.3	1.4	0.0	2.0	0.0	0.0	0.0

	$\Sigma_c^+/\Xi_c^{0,+}(2S, \frac{3}{2}^+)\gamma$			$\Sigma_c^+/\Xi_c^{0,+}(1D, \frac{1}{2}^+)\gamma$			$\Sigma_c^+/\Xi_c^{0,+}(1D, \frac{3}{2}^+)\gamma$			$\Sigma_c^+/\Xi_c^{0,+}(1D, \frac{3}{2}^+)\gamma$		
	Σ_c^+	Ξ_c^0	Ξ_c^+	Σ_c^+	Ξ_c^0	Ξ_c^+	Σ_c^+	Ξ_c^0	Ξ_c^+	Σ_c^+	Ξ_c^0	Ξ_c^+
$\Lambda_c^+/\Xi_c^{0,+}(1F, \frac{5}{2}^-)$	0.0	0.0	0.0	0.0	0.0	0.1	0.0	0.0	0.0	0.0	0.0	0.3
$\Lambda_c^+/\Xi_c^{0,+}(1F, \frac{7}{2}^-)$	0.0	0.0	0.0	0.0	0.0	0.0	0.0	0.0	0.1	0.0	0.0	0.0

	$\Sigma_c^+/\Xi_c^{0,+}(1D, \frac{5}{2}^+)\gamma$			$\Sigma_c^+/\Xi_c^{0,+}(1D, \frac{5}{2}^+)\gamma$			$\Sigma_c^+/\Xi_c^{0,+}(1D, \frac{7}{2}^+)\gamma$		
	Σ_c^+	Ξ_c^0	Ξ_c^+	Σ_c^+	Ξ_c^0	Ξ_c^+	Σ_c^+	Ξ_c^0	Ξ_c^+
$\Lambda_c^+/\Xi_c^{0,+}(1F, \frac{5}{2}^-)$	0.0	0.0	0.0	0.0	0.0	0.5	0.0	0.0	0.0
$\Lambda_c^+/\Xi_c^{0,+}(1F, \frac{7}{2}^-)$	0.0	0.0	0.2	0.0	0.0	0.0	0.0	0.0	0.5

singly charmed baryons in the constituent quark model, *Int. J. Theor. Phys.* **59**, 1129–1156 (2020).

- [34] E. Ortiz-Pacheco and R. Bijker, Masses and radiative decay widths of S - and P -wave singly, doubly, and triply heavy charm and bottom baryons, *Phys. Rev. D* **108**, 054014 (2023).
- [35] A. Hazra, S. Rakshit, and R. Dhir, Radiative $M1$ transitions of heavy baryons: Effective quark mass scheme, *Phys. Rev. D* **104**, 053002 (2021).
- [36] F. L. Wang, S. Q. Luo, and X. Liu, Radiative decays and magnetic moments of the predicted B_c -like molecules, *Phys. Rev. D* **107**, 114017 (2023).
- [37] M. S. Liu, Q. F. Lü, and X. H. Zhong, Triply charmed and bottom baryons in a constituent quark model, *Phys. Rev. D* **101**, 074031 (2020).
- [38] Q. F. Lü, K. L. Wang, L. Y. Xiao, and X. H. Zhong, Mass spectra and radiative transitions of doubly heavy baryons in a relativized quark model, *Phys. Rev. D* **96**, 114006 (2017).
- [39] L. Y. Xiao, K. L. Wang, Q. f. Lu, X. H. Zhong, and S. L. Zhu, Strong and radiative decays of the doubly charmed baryons, *Phys. Rev. D* **96**, 094005 (2017).
- [40] Y. X. Yao, K. L. Wang, and X. H. Zhong, Strong and radiative decays of the low-lying D -wave singly heavy baryons, *Phys. Rev. D* **98**, 076015 (2018).
- [41] K. L. Wang, Y. X. Yao, X. H. Zhong, and Q. Zhao, Strong and radiative decays of the low-lying S - and P -wave singly heavy baryons, *Phys. Rev. D* **96**, 116016 (2017).
- [42] K. L. Wang, L. Y. Xiao, X. H. Zhong, and Q. Zhao, Understanding the newly observed Ω_c states through their decays, *Phys. Rev. D* **95**, 116010 (2017).
- [43] H. Bahtiyar, K. U. Can, G. Erkol, M. Oka, and T. T. Takahashi, $\Xi_c \gamma \rightarrow \Xi_c'$ transition in lattice QCD, *Phys. Lett. B* **772**, 121–126 (2017).
- [44] M. A. Ivanov, J. G. Korner, and V. E. Lyubovitskij, One photon transitions between heavy baryons in a relativistic three quark model, *Phys. Lett. B* **448**, 143–151 (1999).
- [45] M. A. Ivanov, J. G. Korner, V. E. Lyubovitskij, and A. G. Rusetsky, Strong and radiative decays of heavy flavored baryons, *Phys. Rev. D* **60**, 094002 (1999).

TABLE V: Radiative decay widths of $\Sigma_c(1P)/\Xi_c'(1P)\Sigma_c(2S)/\Xi_c'(2S)/\Omega_c(2S)$ decaying into radial or orbital excited states of single-charm baryon.

	$\Lambda_c^+/\Xi_c^{0,+}(1P, \frac{1}{2}^-)\gamma$			$\Lambda_c^+/\Xi_c^{0,+}(1P, \frac{3}{2}^-)\gamma$			$\Lambda_c^+/\Xi_c^{0,+}(2S, \frac{1}{2}^+)\gamma$		
	Λ_c^+	Ξ_c^0	Ξ_c^+	Λ_c^+	Ξ_c^0	Ξ_c^+	Λ_c^+	Ξ_c^0	Ξ_c^+
$\Sigma_{c0}^+/\Xi_{c0}^{0,+}(1P, \frac{1}{2}^-)$	28.4	0.2	7.8	33.0	0.2	7.3	0.0
$\Sigma_{c1}^+/\Xi_{c1}^{0,+}(1P, \frac{1}{2}^-)$	43.7	0.2	11.5	12.2	0.1	2.5	0.0
$\Sigma_{c1}^+/\Xi_{c1}^{0,+}(1P, \frac{3}{2}^-)$	15.3	0.1	5.5	47.7	0.3	14.8	0.0
$\Sigma_{c2}^+/\Xi_{c2}^{0,+}(1P, \frac{3}{2}^-)$	61.3	0.5	22.2	7.2	0.0	2.3	0.0
$\Sigma_{c2}^+/\Xi_{c2}^{0,+}(1P, \frac{5}{2}^-)$	0.1	0.0	0.0	55.9	0.4	21.0	0.0
$\Sigma_c^+/\Xi_c^{0,+}(2S, \frac{1}{2}^+)$	11.7	0.1	4.4	19.5	0.1	6.9	63.0	0.4	18.4
$\Sigma_c^{*+}/\Xi_c^{*0,+}(2S, \frac{3}{2}^+)$	13.3	0.1	5.9	23.9	0.2	9.9	88.1	0.7	35.3

	$\Lambda_c^+/\Xi_c^{0,+}(1D, \frac{3}{2}^+)\gamma$			$\Lambda_c^+/\Xi_c^{0,+}(1D, \frac{5}{2}^+)\gamma$			$\Sigma_{c0}^{0,+,++}/\Xi_{c0}^{0,+}/\Omega_{c0}^0(1P, \frac{1}{2}^-)\gamma$					
	Λ_c^+	Ξ_c^0	Ξ_c^+	Λ_c^+	Ξ_c^0	Ξ_c^+	Σ_c^0	Σ_c^+	Σ_c^{++}	$\Xi_c'^0$	$\Xi_c'^+$	Ω_c^0
$\Sigma_c^{0,+,++}/\Xi_c^{0,+}/\Omega_c^0(2S, \frac{1}{2}^+)$	0.0	0.0	0.0	0.0	0.0	0.0	10.0	0.0	8.4	10.5	0.3	10.0
$\Sigma_c^{0,+,++}/\Xi_c^{0,+}/\Omega_c^0(2S, \frac{3}{2}^+)$	0.0	0.0	0.0	0.0	0.0	0.0	12.3	0.0	10.1	13.4	0.5	13.7

	$\Sigma_{c1}^{0,+,++}/\Xi_{c1}^{0,+}/\Omega_{c1}^0(1P, \frac{1}{2}^-)\gamma$						$\Sigma_{c1}^{0,+,++}/\Xi_{c1}^{0,+}/\Omega_{c1}^0(1P, \frac{3}{2}^-)\gamma$					
	Σ_c^0	Σ_c^+	Σ_c^{++}	$\Xi_c'^0$	$\Xi_c'^+$	Ω_c^0	Σ_c^0	Σ_c^+	Σ_c^{++}	$\Xi_c'^0$	$\Xi_c'^+$	Ω_c^0
$\Sigma_c^{0,+,++}/\Xi_c^{0,+}/\Omega_c^0(2S, \frac{1}{2}^+)$	28.5	0.0	29.6	27.5	0.3	24.0	11.5	0.1	12.4	10.6	0.2	8.6
$\Sigma_c^{0,+,++}/\Xi_c^{0,+}/\Omega_c^0(2S, \frac{3}{2}^+)$	8.9	0.1	10.6	8.7	0.2	8.0	39.3	0.0	40.7	38.1	0.5	34.8

	$\Sigma_c^{0,+,++}/\Xi_c^{0,+}/\Omega_c^0(2S, \frac{1}{2}^+)\gamma$					
	Σ_c^0	Σ_c^+	Σ_c^{++}	$\Xi_c'^0$	$\Xi_c'^+$	Ω_c^0
$\Sigma_c^{0,+,++}/\Xi_c^{0,+}/\Omega_c^0(2S, \frac{1}{2}^+)$	103.0	1.0	145.4	77.8	0.2	51.5
$\Sigma_c^{0,+,++}/\Xi_c^{0,+}/\Omega_c^0(2S, \frac{3}{2}^+)$	14.4	0.3	23.0	11.3	0.2	8.5

	$\Sigma_c^{0,+,++}/\Xi_c^{0,+}/\Omega_c^0(2S, \frac{1}{2}^+)\gamma$					
	Σ_c^0	Σ_c^+	Σ_c^{++}	$\Xi_c'^0$	$\Xi_c'^+$	Ω_c^0
$\Sigma_c^{0,+,++}/\Xi_c^{0,+}/\Omega_c^0(2S, \frac{1}{2}^+)$
$\Sigma_c^{0,+,++}/\Xi_c^{0,+}/\Omega_c^0(2S, \frac{3}{2}^+)$	0.2	0.0	0.2	0.1	0.0	0.2

- [46] S. Q. Luo and X. Liu, Investigating the spectroscopy behavior of undetected $1F$ -wave charmed baryons, *Phys. Rev. D* **108**, 034002 (2023).
- [47] E. Hiyama, Y. Kino, and M. Kamimura, Gaussian expansion method for few-body systems, *Prog. Part. Nucl. Phys.* **51**, 223–307 (2003).
- [48] S. Q. Luo and X. Liu, Newly observed $\Omega_c(3327)$: A good candidate for a D -wave charmed baryon, *Phys. Rev. D* **107**, 074041 (2023).
- [49] J. Kahn (Belle-II Collaboration), The Belle II experiment, 2017, doi:10.23727/CERN-Proceedings-2017-001.45.
- [50] W. Altmannshofer *et al.* (Belle-II Collaboration), The Belle II physics book, *PTEP* **2019**, 123C01 (2019), [Erratum: PTEP 2020, 029201 (2020)].
- [51] P. Di Nezza (LHCb Collaboration), LHC Run 3 and Run 4 prospects for heavy-ion physics with LHCb, *Nucl. Phys. A* **1005**, 121872 (2021).
- [52] S. Belin, LHC Run 3 and Run 4 prospects for heavy-ion physics with LHCb, *PoS HardProbes2020*, 176 (2021).
- [53] F. E. Close and L. A. Copley, Electromagnetic interactions of weakly bound composite systems, *Nucl. Phys. B* **19**, 477–500 (1970).
- [54] Z. P. Li, The Threshold pion photoproduction of nucleons in the chiral quark model, *Phys. Rev. D* **50**, 5639–5646 (1994).
- [55] Z. P. Li, H. X. Ye, and M. H. Lu, An unified approach to pseudoscalar meson photoproductions off nucleons in the quark model, *Phys. Rev. C* **56**, 1099–1113 (1997).
- [56] W. J. Deng, H. Liu, L. C. Gui, and X. H. Zhong, Charmonium spectrum and their electromagnetic transitions with higher multipole contributions, *Phys. Rev. D* **95**, 034026 (2017).
- [57] C. H. Wang, L. Tang, T. Y. Li, G. P. Zheng, J. F. Hu, and C. Q. Pang, The effective β value in a simple harmonic oscillator wave function, *Nucl. Phys. Rev.* **39**, 160–171 (2022).
- [58] B. Chen, K. W. Wei, X. Liu, and T. Matsuki, Low-lying charmed and charmed-strange baryon states, *Eur. Phys. J. C* **77**, 154 (2017).
- [59] B. Chen, K. W. Wei, X. Liu, and A. Zhang, Role of newly discovered $\Xi_b(6227)^-$ for constructing excited bottom baryon family, *Phys. Rev. D* **98**, 031502 (2018).
- [60] W. Roberts and M. Pervin, Heavy baryons in a quark model, *Int. J. Mod. Phys. A* **23**, 2817–2860 (2008).
- [61] D. Ebert, K. G. Klimenko, and V. L. Yudin, Mass spectrum of diquarks and mesons in the color-flavor locked phase of dense quark matter, *Eur. Phys. J. C* **53**, 65–76 (2008).
- [62] D. Ebert, R. N. Faustov, and V. O. Galkin, Spectroscopy and Regge trajectories of heavy baryons in the relativistic quark-diquark picture, *Phys. Rev. D* **84**, 014025 (2011).
- [63] T. Yoshida, E. Hiyama, A. Hosaka, M. Oka, and K. Sadato, Spectrum of heavy baryons in the quark model, *Phys. Rev. D* **92**, 114029 (2015).

TABLE VI: Radiative decay widths of $\Sigma_c(1D)/\Xi'_c(1D)/\Omega_c(1D)$ decaying into radial or orbital excited states of single-charm baryon.

	$\Lambda_c^+/\Xi_c^{0,+}(1P, \frac{1}{2}^-)\gamma$			$\Lambda_c^+/\Xi_c^{0,+}(1P, \frac{3}{2}^-)\gamma$			$\Lambda_c^+/\Xi_c^{0,+}(2S, \frac{1}{2}^+)\gamma$		
	Λ_c^+	Ξ_c^0	Ξ_c^+	Λ_c^+	Ξ_c^0	Ξ_c^+	Λ_c^+	Ξ_c^0	Ξ_c^+
$\Sigma_{c1}^+/\Xi_{c1}^{\prime 0,+}(1D, \frac{1}{2}^+)$	38.7	0.2	16.1	19.7	0.1	7.6	0.4	0.0	0.0
$\Sigma_{c1}^+/\Xi_{c1}^{\prime 0,+}(1D, \frac{3}{2}^+)$	13.1	0.1	5.4	45.6	0.3	19.2	0.6	0.0	0.1
$\Sigma_{c2}^+/\Xi_{c2}^{\prime 0,+}(1D, \frac{3}{2}^+)$	86.4	0.6	38.1	20.4	0.1	8.7	1.0	0.0	0.1
$\Sigma_{c2}^+/\Xi_{c2}^{\prime 0,+}(1D, \frac{5}{2}^+)$	4.6	0.0	2.0	94.8	0.7	42.4	1.4	0.0	0.2
$\Sigma_{c3}^+/\Xi_{c3}^{\prime 0,+}(1D, \frac{5}{2}^+)$	48.8	0.3	23.0	11.4	0.1	5.3	0.4	0.0	0.0
$\Sigma_{c3}^+/\Xi_{c3}^{\prime 0,+}(1D, \frac{7}{2}^+)$	0.3	0.0	0.0	53.0	0.4	25.2	0.4	0.0	0.1

	$\Lambda_c^+/\Xi_c^{0,+}(1D, \frac{3}{2}^+)\gamma$			$\Lambda_c^+/\Xi_c^{0,+}(1D, \frac{5}{2}^+)\gamma$			$\Sigma_{c0}^{0,+++}/\Xi_{c0}^{\prime 0,+}/\Omega_{c0}^0(1P, \frac{1}{2}^-)\gamma$					
	Λ_c^+	Ξ_c^0	Ξ_c^+	Λ_c^+	Ξ_c^0	Ξ_c^+	Σ_c^0	Σ_c^+	Σ_c^{++}	$\Xi_c^{\prime 0}$	$\Xi_c^{\prime +}$	Ω_c^0
$\Sigma_{c1}^{0,+++}/\Xi_{c1}^{\prime 0,+}/\Omega_{c1}^0(1D, \frac{1}{2}^+)$	71.0	0.5	23.5	0.0	0.0	0.0	242.8	0.9	306.3	217.3	0.1	187.7
$\Sigma_{c1}^{0,+++}/\Xi_{c1}^{\prime 0,+}/\Omega_{c1}^0(1D, \frac{3}{2}^+)$	8.5	0.1	3.2	55.4	0.4	19.3	260.8	2.1	361.3	231.6	0.1	203.1
$\Sigma_{c2}^{0,+++}/\Xi_{c2}^{\prime 0,+}/\Omega_{c2}^0(1D, \frac{3}{2}^+)$	50.2	0.4	18.7	3.9	0.0	1.3	2.1	0.5	8.4	1.3	0.9	0.7
$\Sigma_{c2}^{0,+++}/\Xi_{c2}^{\prime 0,+}/\Omega_{c2}^0(1D, \frac{5}{2}^+)$	4.3	0.0	1.8	43.4	0.3	16.8	2.5	0.6	10.1	1.6	1.1	0.9
$\Sigma_{c3}^{0,+++}/\Xi_{c3}^{\prime 0,+}/\Omega_{c3}^0(1D, \frac{5}{2}^+)$	38.7	0.3	16.0	1.8	0.0	0.7	0.1	0.0	0.3	0.1	0.0	0.1
$\Sigma_{c3}^{0,+++}/\Xi_{c3}^{\prime 0,+}/\Omega_{c3}^0(1D, \frac{7}{2}^+)$	0.0	0.0	0.0	30.3	0.3	12.6	0.1	0.0	0.4	0.1	0.0	0.1

	$\Sigma_{c1}^{0,+++}/\Xi_{c1}^{\prime 0,+}/\Omega_{c1}^0(1P, \frac{1}{2}^-)\gamma$						$\Sigma_{c1}^{0,+++}/\Xi_{c1}^{\prime 0,+}/\Omega_{c1}^0(1P, \frac{3}{2}^-)\gamma$					
	Σ_c^0	Σ_c^+	Σ_c^{++}	$\Xi_c^{\prime 0}$	$\Xi_c^{\prime +}$	Ω_c^0	Σ_c^0	Σ_c^+	Σ_c^{++}	$\Xi_c^{\prime 0}$	$\Xi_c^{\prime +}$	Ω_c^0
$\Sigma_{c1}^{0,+++}/\Xi_{c1}^{\prime 0,+}/\Omega_{c1}^0(1D, \frac{1}{2}^+)$	165.4	2.4	254.1	137.3	0.6	109.7	71.0	0.8	101.8	57.6	0.3	44.4
$\Sigma_{c1}^{0,+++}/\Xi_{c1}^{\prime 0,+}/\Omega_{c1}^0(1D, \frac{3}{2}^+)$	45.3	1.1	77.7	37.1	0.5	29.9	193.7	3.0	298.8	157.2	1.1	124.9
$\Sigma_{c2}^{0,+++}/\Xi_{c2}^{\prime 0,+}/\Omega_{c2}^0(1D, \frac{3}{2}^+)$	220.7	0.5	244.4	216.1	2.2	206.0	39.1	0.4	43.5	37.5	0.9	34.9
$\Sigma_{c2}^{0,+++}/\Xi_{c2}^{\prime 0,+}/\Omega_{c2}^0(1D, \frac{5}{2}^+)$	0.7	0.5	4.9	0.3	0.7	0.1	236.5	0.8	285.2	225.1	1.1	210.4
$\Sigma_{c3}^{0,+++}/\Xi_{c3}^{\prime 0,+}/\Omega_{c3}^0(1D, \frac{5}{2}^+)$	1.7	0.4	6.5	1.2	0.8	0.8	0.4	0.1	1.4	0.3	0.1	0.2
$\Sigma_{c3}^{0,+++}/\Xi_{c3}^{\prime 0,+}/\Omega_{c3}^0(1D, \frac{7}{2}^+)$	0.1	0.0	0.3	0.1	0.0	0.1	1.6	0.4	6.2	1.1	0.7	0.7

	$\Sigma_{c2}^{0,+++}/\Xi_{c2}^{\prime 0,+}/\Omega_{c2}^0(1P, \frac{3}{2}^-)\gamma$						$\Sigma_{c2}^{0,+++}/\Xi_{c2}^{\prime 0,+}/\Omega_{c2}^0(1P, \frac{5}{2}^-)\gamma$					
	Σ_c^0	Σ_c^+	Σ_c^{++}	$\Xi_c^{\prime 0}$	$\Xi_c^{\prime +}$	Ω_c^0	Σ_c^0	Σ_c^+	Σ_c^{++}	$\Xi_c^{\prime 0}$	$\Xi_c^{\prime +}$	Ω_c^0
$\Sigma_{c1}^{0,+++}/\Xi_{c1}^{\prime 0,+}/\Omega_{c1}^0(1D, \frac{1}{2}^+)$	23.6	1.0	46.0	16.2	0.7	10.4	1.7	0.3	5.6	0.6	0.1	0.2
$\Sigma_{c1}^{0,+++}/\Xi_{c1}^{\prime 0,+}/\Omega_{c1}^0(1D, \frac{3}{2}^+)$	4.5	0.5	12.0	2.5	0.2	1.5	23.2	1.0	44.9	15.6	0.6	10.2
$\Sigma_{c2}^{0,+++}/\Xi_{c2}^{\prime 0,+}/\Omega_{c2}^0(1D, \frac{3}{2}^+)$	116.7	1.7	179.3	94.6	0.4	74.0	12.6	0.1	17.5	10.1	0.0	7.8
$\Sigma_{c2}^{0,+++}/\Xi_{c2}^{\prime 0,+}/\Omega_{c2}^0(1D, \frac{5}{2}^+)$	9.4	0.3	17.4	7.3	0.1	5.7	121.4	1.8	186.3	97.6	0.4	76.5
$\Sigma_{c3}^{0,+++}/\Xi_{c3}^{\prime 0,+}/\Omega_{c3}^0(1D, \frac{5}{2}^+)$	216.0	1.0	206.0	227.0	6.7	231.2	15.3	0.3	14.3	16.1	0.9	16.4
$\Sigma_{c3}^{0,+++}/\Xi_{c3}^{\prime 0,+}/\Omega_{c3}^0(1D, \frac{7}{2}^+)$	0.2	0.3	2.4	0.1	0.5	0.0	213.3	0.5	221.1	219.6	4.2	220.5

	$\Sigma_c^{0,+++}/\Xi_c^{0,+}/\Omega_c^0(2S, \frac{1}{2}^+)\gamma$						$\Sigma_c^{*0,+++}/\Xi_c^{*0,+}/\Omega_c^{*0}(2S, \frac{3}{2}^+)\gamma$					
	Σ_c^0	Σ_c^+	Σ_c^{++}	$\Xi_c^{\prime 0}$	$\Xi_c^{\prime +}$	Ω_c^0	Σ_c^0	Σ_c^+	Σ_c^{++}	$\Xi_c^{\prime 0}$	$\Xi_c^{\prime +}$	Ω_c^0
$\Sigma_{c1}^{0,+++}/\Xi_{c1}^{\prime 0,+}/\Omega_{c1}^0(1D, \frac{1}{2}^+)$	0.0	0.0	0.0	0.0	0.0	0.0	0.0	0.0	0.2	0.0	0.0	0.0
$\Sigma_{c1}^{0,+++}/\Xi_{c1}^{\prime 0,+}/\Omega_{c1}^0(1D, \frac{3}{2}^+)$	0.2	0.1	1.3	0.1	0.1	0.0	0.0	0.0	0.3	0.0	0.0	0.0
$\Sigma_{c2}^{0,+++}/\Xi_{c2}^{\prime 0,+}/\Omega_{c2}^0(1D, \frac{3}{2}^+)$	0.0	0.0	0.3	0.0	0.0	0.0	0.0	0.0	0.0	0.0	0.0	0.0
$\Sigma_{c2}^{0,+++}/\Xi_{c2}^{\prime 0,+}/\Omega_{c2}^0(1D, \frac{5}{2}^+)$	0.0	0.0	0.3	0.0	0.0	0.0	0.0	0.0	0.1	0.0	0.0	0.0
$\Sigma_{c3}^{0,+++}/\Xi_{c3}^{\prime 0,+}/\Omega_{c3}^0(1D, \frac{5}{2}^+)$	0.0	0.0	0.1	0.0	0.0	0.0	0.0	0.0	0.0	0.0	0.0	0.0
$\Sigma_{c3}^{0,+++}/\Xi_{c3}^{\prime 0,+}/\Omega_{c3}^0(1D, \frac{7}{2}^+)$	0.0	0.0	0.0	0.0	0.0	0.0	0.0	0.0	0.0	0.0	0.0	0.0

[64] Z. Shah, K. Thakkar, A. K. Rai, and P. C. Vinodkumar, Mass spectra and Regge trajectories of Λ_c^+ , Σ_c^0 , Ξ_c^0 and Ω_c^0 baryons, *Chin. Phys. C* **40**, 123102 (2016).

[65] G. L. Yu, Z. Y. Li, Z. G. Wang, J. Lu, and M. Yan, Systematic analysis of single heavy baryons Λ_Q , Σ_Q and Ω_Q , *Nucl. Phys. B*

990, 116183 (2023).

[66] H. Garcia-Tecocoatz, A. Giachino, J. Li, A. Ramirez-Morales, and E. Santopinto, Strong decay widths and mass spectra of charmed baryons, *Phys. Rev. D* **107**, 034031 (2023).

[67] R. Aaij *et al.* (LHCb Collaboration), Observation of new Ξ_c^0

TABLE VII: Radiative decay widths of $\Sigma_c(1F)/\Xi_c(1F)/\Omega_c(1F)$ decaying into radial or orbital excited states of single-charm baryon.

	$\Lambda_c^+/\Xi_c^{0,+}(1P, \frac{1}{2}^-)\gamma$			$\Lambda_c^+/\Xi_c^{0,+}(1P, \frac{3}{2}^-)\gamma$			$\Lambda_c^+/\Xi_c^{0,+}(2S, \frac{1}{2}^+)\gamma$		
	Λ_c^+	Ξ_c^0	Ξ_c^+	Λ_c^+	Ξ_c^0	Ξ_c^+	Λ_c^+	Ξ_c^0	Ξ_c^+
$\Sigma_{c2}^+/\Xi_{c2}^{0,+}(1F, \frac{3}{2}^-)$	23.3	0.1	9.5	10.3	0.0	3.9	2.0	0.0	0.3
$\Sigma_{c2}^+/\Xi_{c2}^{0,+}(1F, \frac{5}{2}^-)$	3.6	0.0	1.3	29.4	0.1	11.8	2.3	0.0	0.3
$\Sigma_{c3}^+/\Xi_{c3}^{0,+}(1F, \frac{5}{2}^-)$	45.9	0.1	19.1	14.6	0.0	5.8	3.6	0.0	0.6
$\Sigma_{c3}^+/\Xi_{c3}^{0,+}(1F, \frac{7}{2}^-)$	1.6	0.0	0.5	56.5	0.2	23.3	3.9	0.0	0.6
$\Sigma_{c4}^+/\Xi_{c4}^{0,+}(1F, \frac{7}{2}^-)$	22.0	0.1	9.4	7.0	0.0	2.9	1.1	0.0	0.2
$\Sigma_{c4}^+/\Xi_{c4}^{0,+}(1F, \frac{9}{2}^-)$	0.3	0.0	0.0	26.8	0.1	11.4	1.2	0.0	0.2

	$\Lambda_c^+/\Xi_c^{0,+}(1D, \frac{3}{2}^+)\gamma$			$\Lambda_c^+/\Xi_c^{0,+}(1D, \frac{5}{2}^+)\gamma$			$\Lambda_c^+/\Xi_c^{0,+}(1F, \frac{5}{2}^-)\gamma$			$\Lambda_c^+/\Xi_c^{0,+}(1F, \frac{7}{2}^-)\gamma$		
	Λ_c^+	Ξ_c^0	Ξ_c^+	Λ_c^+	Ξ_c^0	Ξ_c^+	Λ_c^+	Ξ_c^0	Ξ_c^+	Λ_c^+	Ξ_c^0	Ξ_c^+
$\Sigma_{c2}^{0,+,++}/\Xi_{c2}^{0,+}/\Omega_{c2}^0(1F, \frac{3}{2}^-)$	75.4	0.5	34.1	9.5	0.1	4.0	80.4	0.5	25.6	0.1	0.0	0.0
$\Sigma_{c2}^{0,+,++}/\Xi_{c2}^{0,+}/\Omega_{c2}^0(1F, \frac{5}{2}^-)$	7.6	0.0	3.3	71.4	0.5	32.3	4.2	0.0	1.4	78.5	0.5	25.9
$\Sigma_{c3}^{0,+,++}/\Xi_{c3}^{0,+}/\Omega_{c3}^0(1F, \frac{5}{2}^-)$	99.4	0.7	47.4	9.1	0.1	4.3	48.7	0.3	15.7	2.3	0.0	0.7
$\Sigma_{c3}^{0,+,++}/\Xi_{c3}^{0,+}/\Omega_{c3}^0(1F, \frac{7}{2}^-)$	2.6	0.0	1.2	94.6	0.7	45.3	1.9	0.0	0.6	49.7	0.3	16.4
$\Sigma_{c4}^{0,+,++}/\Xi_{c4}^{0,+}/\Omega_{c4}^0(1F, \frac{7}{2}^-)$	50.1	0.4	25.1	4.6	0.0	2.3	27.1	0.2	8.1	0.9	0.0	0.3
$\Sigma_{c4}^{0,+,++}/\Xi_{c4}^{0,+}/\Omega_{c4}^0(1F, \frac{9}{2}^-)$	0.1	0.0	0.0	45.9	0.4	23.1	0.0	0.0	0.0	26.9	0.2	7.8

	$\Sigma_{c0}^{0,+,++}/\Xi_{c0}^{0,+}/\Omega_{c0}^0(1P, \frac{1}{2}^-)\gamma$						$\Sigma_{c1}^{0,+,++}/\Xi_{c1}^{0,+}/\Omega_{c1}^0(1P, \frac{1}{2}^-)\gamma$					
	Σ_c^0	Σ_c^+	Σ_c^{++}	Ξ_c^0	Ξ_c^+	Ω_c^0	Σ_c^0	Σ_c^+	Σ_c^{++}	Ξ_c^0	Ξ_c^+	Ω_c^0
$\Sigma_{c2}^{0,+,++}/\Xi_{c2}^{0,+}/\Omega_{c2}^0(1F, \frac{3}{2}^-)$	66.2	56.6	537.5	29.5	40.5	11.2	46.3	34.6	344.1	20.8	24.2	8.1
$\Sigma_{c2}^{0,+,++}/\Xi_{c2}^{0,+}/\Omega_{c2}^0(1F, \frac{5}{2}^-)$	70.6	54.9	539.0	33.0	37.6	13.7	21.3	14.8	151.8	10.0	10.0	4.2
$\Sigma_{c3}^{0,+,++}/\Xi_{c3}^{0,+}/\Omega_{c3}^0(1F, \frac{5}{2}^-)$	1.7	0.4	7.0	0.9	0.5	0.4	43.9	43.8	393.8	20.2	31.3	7.9
$\Sigma_{c3}^{0,+,++}/\Xi_{c3}^{0,+}/\Omega_{c3}^0(1F, \frac{7}{2}^-)$	1.8	0.4	7.2	0.9	0.5	0.4	1.6	0.3	5.5	0.7	0.1	0.4
$\Sigma_{c4}^{0,+,++}/\Xi_{c4}^{0,+}/\Omega_{c4}^0(1F, \frac{7}{2}^-)$	0.2	0.1	1.1	0.1	0.0	0.0	1.5	0.4	6.2	0.8	0.4	0.4
$\Sigma_{c4}^{0,+,++}/\Xi_{c4}^{0,+}/\Omega_{c4}^0(1F, \frac{9}{2}^-)$	0.2	0.1	1.1	0.1	0.0	0.0	0.2	0.1	0.8	0.1	0.0	0.0

	$\Sigma_{c1}^{0,+,++}/\Xi_{c1}^{0,+}/\Omega_{c1}^0(1P, \frac{3}{2}^-)\gamma$						$\Sigma_{c2}^{0,+,++}/\Xi_{c2}^{0,+}/\Omega_{c2}^0(1P, \frac{3}{2}^-)\gamma$					
	Σ_c^0	Σ_c^+	Σ_c^{++}	Ξ_c^0	Ξ_c^+	Ω_c^0	Σ_c^0	Σ_c^+	Σ_c^{++}	Ξ_c^0	Ξ_c^+	Ω_c^0
$\Sigma_{c2}^{0,+,++}/\Xi_{c2}^{0,+}/\Omega_{c2}^0(1F, \frac{3}{2}^-)$	42.8	33.5	327.9	18.4	23.9	6.7	15.0	9.4	99.9	6.4	6.4	2.3
$\Sigma_{c2}^{0,+,++}/\Xi_{c2}^{0,+}/\Omega_{c2}^0(1F, \frac{5}{2}^-)$	72.0	51.1	518.4	32.3	35.3	12.7	9.0	4.0	48.6	3.1	2.1	1.0
$\Sigma_{c3}^{0,+,++}/\Xi_{c3}^{0,+}/\Omega_{c3}^0(1F, \frac{5}{2}^-)$	13.9	12.6	116.0	6.1	9.2	2.3	42.2	31.7	314.3	18.8	22.4	7.3
$\Sigma_{c3}^{0,+,++}/\Xi_{c3}^{0,+}/\Omega_{c3}^0(1F, \frac{7}{2}^-)$	59.3	51.8	487.6	28.2	36.1	11.8	6.4	4.0	42.3	2.9	2.5	1.2
$\Sigma_{c4}^{0,+,++}/\Xi_{c4}^{0,+}/\Omega_{c4}^0(1F, \frac{7}{2}^-)$	0.6	0.2	2.6	0.3	0.1	0.1	41.1	47.7	407.2	19.3	34.3	7.6
$\Sigma_{c4}^{0,+,++}/\Xi_{c4}^{0,+}/\Omega_{c4}^0(1F, \frac{9}{2}^-)$	1.8	0.5	7.2	0.9	0.5	0.4	0.6	0.1	1.6	0.4	0.0	0.2

	$\Sigma_{c2}^{0,+,++}/\Xi_{c2}^{0,+}/\Omega_{c2}^0(1P, \frac{5}{2}^-)\gamma$					
	Σ_c^0	Σ_c^+	Σ_c^{++}	Ξ_c^0	Ξ_c^+	Ω_c^0
$\Sigma_{c2}^{0,+,++}/\Xi_{c2}^{0,+}/\Omega_{c2}^0(1F, \frac{3}{2}^-)$	11.6	5.8	66.8	3.8	3.3	1.1
$\Sigma_{c2}^{0,+,++}/\Xi_{c2}^{0,+}/\Omega_{c2}^0(1F, \frac{5}{2}^-)$	19.4	11.5	124.5	7.8	7.6	2.8
$\Sigma_{c3}^{0,+,++}/\Xi_{c3}^{0,+}/\Omega_{c3}^0(1F, \frac{5}{2}^-)$	10.7	8.4	81.6	4.4	5.9	1.5
$\Sigma_{c3}^{0,+,++}/\Xi_{c3}^{0,+}/\Omega_{c3}^0(1F, \frac{7}{2}^-)$	48.6	35.1	353.4	21.7	24.5	8.5
$\Sigma_{c4}^{0,+,++}/\Xi_{c4}^{0,+}/\Omega_{c4}^0(1F, \frac{7}{2}^-)$	4.9	5.6	47.5	2.2	4.2	0.8
$\Sigma_{c4}^{0,+,++}/\Xi_{c4}^{0,+}/\Omega_{c4}^0(1F, \frac{9}{2}^-)$	48.3	49.4	440.0	23.7	34.7	10.2

–Continue.–

- baryons decaying to $\Lambda_c^+ K^-$, *Phys. Rev. Lett.* **124**, 222001 (2020).
- [68] R. Aaij *et al.* (LHCb Collaboration), Study of the $B^- \rightarrow \Lambda_c^+ \bar{\Lambda}_c^- K^-$ decay, *Phys. Rev. D* **108**, 012020 (2023).
- [69] R. Aaij *et al.* (LHCb Collaboration), Observation of five new narrow Ω_c^0 states decaying to $\Xi_c^+ K^-$, *Phys. Rev. Lett.* **118**, 182001 (2017).
- [70] S. S. Agaev, K. Azizi, and H. Sundu, On the nature of the newly

–Continue.–

	$\Sigma_c^{0,+,++}/\Xi_c^{\prime 0,+}/\Omega_c^0(2S, \frac{1}{2}^+)\gamma$						$\Sigma_c^{0,+,++}/\Xi_c^{\prime 0,+}/\Omega_c^0(2S, \frac{3}{2}^+)\gamma$					
	Σ_c^0	Σ_c^+	Σ_c^{++}	$\Xi_c^{\prime 0}$	$\Xi_c^{\prime +}$	Ω_c^0	Σ_c^0	Σ_c^+	Σ_c^{++}	$\Xi_c^{\prime 0}$	$\Xi_c^{\prime +}$	Ω_c^0
$\Sigma_{c2}^{0,+,++}/\Xi_{c2}^{\prime 0,+}/\Omega_{c2}^0(1F, \frac{3}{2}^-)$	0.0	0.0	0.1	0.0	0.0	0.0	7.6	1.2	24.8	3.2	0.3	1.5
$\Sigma_{c2}^{0,+,++}/\Xi_{c2}^{\prime 0,+}/\Omega_{c2}^0(1F, \frac{5}{2}^-)$	7.6	1.2	24.8	3.4	0.3	1.7	4.0	0.7	13.0	1.7	0.1	0.8
$\Sigma_{c3}^{0,+,++}/\Xi_{c3}^{\prime 0,+}/\Omega_{c3}^0(1F, \frac{5}{2}^-)$	2.6	0.4	8.5	1.5	0.1	1.0	2.0	0.3	6.4	1.1	0.1	0.7
$\Sigma_{c3}^{0,+,++}/\Xi_{c3}^{\prime 0,+}/\Omega_{c3}^0(1F, \frac{7}{2}^-)$	1.7	0.3	5.4	0.9	0.1	0.6	3.0	0.5	9.8	1.6	0.1	1.0
$\Sigma_{c4}^{0,+,++}/\Xi_{c4}^{\prime 0,+}/\Omega_{c4}^0(1F, \frac{7}{2}^-)$	1.6	0.2	4.9	1.3	0.1	1.2	0.3	0.0	0.9	0.2	0.0	0.2
$\Sigma_{c4}^{0,+,++}/\Xi_{c4}^{\prime 0,+}/\Omega_{c4}^0(1F, \frac{9}{2}^-)$	0.0	0.0	0.0	0.0	0.0	0.0	1.2	0.2	3.8	1.0	0.1	0.9
	$\Sigma_{c2}^{0,+,++}/\Xi_{c2}^{\prime 0,+}/\Omega_{c2}^0(1D, \frac{1}{2}^+)\gamma$						$\Sigma_{c2}^{0,+,++}/\Xi_{c2}^{\prime 0,+}/\Omega_{c2}^0(1D, \frac{3}{2}^+)\gamma$					
	Σ_c^0	Σ_c^+	Σ_c^{++}	$\Xi_c^{\prime 0}$	$\Xi_c^{\prime +}$	Ω_c^0	Σ_c^0	Σ_c^+	Σ_c^{++}	$\Xi_c^{\prime 0}$	$\Xi_c^{\prime +}$	Ω_c^0
$\Sigma_{c2}^{0,+,++}/\Xi_{c2}^{\prime 0,+}/\Omega_{c2}^0(1F, \frac{3}{2}^-)$	391.7	1.7	501.0	352.2	0.1	306.6	73.2	0.2	87.5	66.3	0.2	56.7
$\Sigma_{c2}^{0,+,++}/\Xi_{c2}^{\prime 0,+}/\Omega_{c2}^0(1F, \frac{5}{2}^-)$	0.7	0.0	1.2	0.5	0.0	0.3	432.9	3.4	592.2	382.1	0.5	327.0
$\Sigma_{c3}^{0,+,++}/\Xi_{c3}^{\prime 0,+}/\Omega_{c3}^0(1F, \frac{5}{2}^-)$	2.2	0.5	8.6	1.5	1.0	0.9	0.5	0.1	2.1	0.4	0.2	0.2
$\Sigma_{c3}^{0,+,++}/\Xi_{c3}^{\prime 0,+}/\Omega_{c3}^0(1F, \frac{7}{2}^-)$	0.1	0.0	0.2	0.0	0.0	0.0	2.4	0.6	9.4	1.6	1.1	0.9
$\Sigma_{c4}^{0,+,++}/\Xi_{c4}^{\prime 0,+}/\Omega_{c4}^0(1F, \frac{7}{2}^-)$	0.0	0.0	0.0	0.0	0.0	0.0	0.0	0.0	0.0	0.0	0.0	0.0
$\Sigma_{c4}^{0,+,++}/\Xi_{c4}^{\prime 0,+}/\Omega_{c4}^0(1F, \frac{9}{2}^-)$	0.0	0.0	0.0	0.0	0.0	0.0	0.0	0.0	0.0	0.0	0.0	0.0
	$\Sigma_{c3}^{0,+,++}/\Xi_{c3}^{\prime 0,+}/\Omega_{c3}^0(1D, \frac{3}{2}^+)\gamma$						$\Sigma_{c3}^{0,+,++}/\Xi_{c3}^{\prime 0,+}/\Omega_{c3}^0(1D, \frac{5}{2}^+)\gamma$					
	Σ_c^0	Σ_c^+	Σ_c^{++}	$\Xi_c^{\prime 0}$	$\Xi_c^{\prime +}$	Ω_c^0	Σ_c^0	Σ_c^+	Σ_c^{++}	$\Xi_c^{\prime 0}$	$\Xi_c^{\prime +}$	Ω_c^0
$\Sigma_{c2}^{0,+,++}/\Xi_{c2}^{\prime 0,+}/\Omega_{c2}^0(1F, \frac{3}{2}^-)$	132.0	3.0	221.3	100.7	1.5	73.5	15.4	0.3	24.5	11.5	0.2	8.2
$\Sigma_{c2}^{0,+,++}/\Xi_{c2}^{\prime 0,+}/\Omega_{c2}^0(1F, \frac{5}{2}^-)$	10.8	0.5	22.0	7.7	0.3	5.5	132.9	3.3	224.4	100.1	1.8	72.7
$\Sigma_{c3}^{0,+,++}/\Xi_{c3}^{\prime 0,+}/\Omega_{c3}^0(1F, \frac{5}{2}^-)$	328.1	0.5	367.1	317.5	2.1	295.4	22.9	0.1	23.0	22.5	0.4	20.9
$\Sigma_{c3}^{0,+,++}/\Xi_{c3}^{\prime 0,+}/\Omega_{c3}^0(1F, \frac{7}{2}^-)$	0.1	0.2	1.0	0.0	0.2	0.0	324.1	0.8	388.3	308.1	0.9	282.7
$\Sigma_{c4}^{0,+,++}/\Xi_{c4}^{\prime 0,+}/\Omega_{c4}^0(1F, \frac{7}{2}^-)$	1.2	0.3	4.7	1.0	0.6	0.7	0.1	0.0	0.4	0.1	0.1	0.1
$\Sigma_{c4}^{0,+,++}/\Xi_{c4}^{\prime 0,+}/\Omega_{c4}^0(1F, \frac{9}{2}^-)$	0.0	0.0	0.0	0.0	0.0	0.0	1.0	0.3	4.1	0.9	0.6	0.6
	$\Sigma_{c4}^{0,+,++}/\Xi_{c4}^{\prime 0,+}/\Omega_{c4}^0(1D, \frac{5}{2}^+)\gamma$						$\Sigma_{c4}^{0,+,++}/\Xi_{c4}^{\prime 0,+}/\Omega_{c4}^0(1D, \frac{7}{2}^+)\gamma$					
	Σ_c^0	Σ_c^+	Σ_c^{++}	$\Xi_c^{\prime 0}$	$\Xi_c^{\prime +}$	Ω_c^0	Σ_c^0	Σ_c^+	Σ_c^{++}	$\Xi_c^{\prime 0}$	$\Xi_c^{\prime +}$	Ω_c^0
$\Sigma_{c2}^{0,+,++}/\Xi_{c2}^{\prime 0,+}/\Omega_{c2}^0(1F, \frac{3}{2}^-)$	9.6	0.7	22.0	5.6	0.5	3.1	0.4	0.1	1.3	0.1	0.0	0.0
$\Sigma_{c2}^{0,+,++}/\Xi_{c2}^{\prime 0,+}/\Omega_{c2}^0(1F, \frac{5}{2}^-)$	0.8	0.1	2.4	0.4	0.1	0.2	9.7	0.7	21.7	5.7	0.5	3.2
$\Sigma_{c3}^{0,+,++}/\Xi_{c3}^{\prime 0,+}/\Omega_{c3}^0(1F, \frac{5}{2}^-)$	93.1	2.0	154.7	70.2	0.8	50.4	5.2	0.1	7.6	3.9	0.0	2.8
$\Sigma_{c3}^{0,+,++}/\Xi_{c3}^{\prime 0,+}/\Omega_{c3}^0(1F, \frac{7}{2}^-)$	3.6	0.2	7.5	2.5	0.1	1.8	94.6	2.1	157.4	70.8	0.9	50.9
$\Sigma_{c4}^{0,+,++}/\Xi_{c4}^{\prime 0,+}/\Omega_{c4}^0(1F, \frac{7}{2}^-)$	264.0	0.8	259.9	274.8	6.0	273.1	10.5	0.2	9.3	11.2	0.6	11.3
$\Sigma_{c4}^{0,+,++}/\Xi_{c4}^{\prime 0,+}/\Omega_{c4}^0(1F, \frac{9}{2}^-)$	0.1	0.2	1.2	0.0	0.3	0.0	256.4	0.4	270.3	262.6	3.8	258.3

discovered Ω states, [EPL **118**, 61001 \(2017\)](#).

- [71] S. S. Agaev, K. Azizi, and H. Sundu, Interpretation of the new Ω_c^0 states via their mass and width, [Eur. Phys. J. C **77**, 395 \(2017\)](#).
- [72] A. Ali, L. Maiani, A. V. Borisov, I. Ahmed, M. Jamil Aslam, A. Y. Parkhomenko, A. D. Polosa, and A. Rehman, A new look at the Y tetraquarks and Ω_c baryons in the diquark model, [Eur. Phys. J. C **78**, 29 \(2018\)](#).
- [73] H. X. Chen, Q. Mao, W. Chen, A. Hosaka, X. Liu, and S. L. Zhu, Decay properties of P -wave charmed baryons from light-cone QCD sum rules, [Phys. Rev. D **95**, 094008 \(2017\)](#).
- [74] B. Chen and X. Liu, New Ω_c^0 baryons discovered by LHCb as the members of $1P$ and $2S$ states, [Phys. Rev. D **96**, 094015 \(2017\)](#).
- [75] H. Y. Cheng and C. W. Chiang, Quantum numbers of Ω_c states and other charmed baryons, [Phys. Rev. D **95**, 094018 \(2017\)](#).
- [76] M. Karliner and J. L. Rosner, Very narrow excited Ω_c baryons, [Phys. Rev. D **95**, 114012 \(2017\)](#).
- [77] M. Padmanath and N. Mathur, Quantum Numbers of Recently Discovered Ω_c^0 Baryons from Lattice QCD, [Phys. Rev. Lett. **119**, 042001 \(2017\)](#).
- [78] W. Wang and R. L. Zhu, Interpretation of the newly observed Ω_c^0 resonances, [Phys. Rev. D **96**, 014024 \(2017\)](#).
- [79] Z. G. Wang, Analysis of $\Omega_c(3000)$, $\Omega_c(3050)$, $\Omega_c(3066)$, $\Omega_c(3090)$ and $\Omega_c(3119)$ with QCD sum rules, [Eur. Phys. J. C **77**, 325 \(2017\)](#).
- [80] H. M. Yang and H. X. Chen, P -wave bottom baryons of the $SU(3)$ flavor $\mathbf{6}_F$, [Phys. Rev. D **101**, 114013 \(2020\)](#), [Erratum: [Phys.Rev.D **102**, 079901 \(2020\)](#)].
- [81] G. Yang, J. Ping, and J. Segovia, The S - and P -wave low-lying baryons in the chiral quark model, [Few Body Syst. **59**, 113 \(2018\)](#).
- [82] Z. Zhao, D. D. Ye, and A. Zhang, Hadronic decay properties of newly observed Ω_c baryons, [Phys. Rev. D **95**, 114024 \(2017\)](#).

- [83] R. Aaij *et al.* (LHCb Collaboration), Observation of New Ω_c^0 states decaying to the $\Xi_c^+ K^-$ final state, *Phys. Rev. Lett.* **131**, 131902 (2023).
- [84] J. Yelton *et al.* (Belle Collaboration), Observation of Excited Ω_c Charmed Baryons in $e^+ e^-$ Collisions, *Phys. Rev. D* **97**, 051102 (2018).
- [85] R. Aaij *et al.* (LHCb Collaboration), Observation of excited Ω_c^0 baryons in $\Omega_b^- \rightarrow \Xi_c^+ K^- \pi^-$ decays, *Phys. Rev. D* **104**, L091102 (2021).
- [86] G. L. Yu, Y. Meng, Z. Y. Li, Z. G. Wang, and L. Jie, Strong decay properties of single heavy baryons Λ_Q , Σ_Q and Ω_Q , *Int. J. Mod. Phys. A* **38**, 2350082 (2023).
- [87] Z. G. Wang, F. Lu, and Y. Liu, Analysis of the D -wave Σ -type charmed baryon states with the QCD sum rules, *Eur. Phys. J. C* **83**, 689 (2023).
- [88] M. Karliner and J. L. Rosner, Excited Ω_c baryons as $2S$ states, *Phys. Rev. D* **108**, 014006 (2023).
- [89] J. H. Pan and J. Pan, Investigation of the mass spectra of singly heavy baryons Σ_Q , Ξ'_Q , and Ω_Q ($Q = c, b$) in the Regge trajectory model, *Phys. Rev. D* **109**, 076010 (2024).